LOS ALAMOS SCIENTIFIC LABORATORY
of the
University of California
LOS ALAMOS • NEW MEXICO

# Computation of Fast Neutron Penetration in Air by the "Sn-Method" with Special Emphasis on the Use of "Multitable-Multigroup Cross Section Sets"

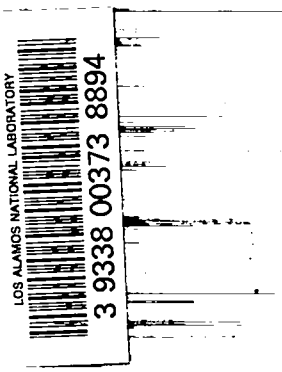


UNITED STATES
ATOMIC ENERGY COMMISSION
CONTRACT W-7405-ENG. 36

This report expresses the opinions of the author or authors and does not necessarily reflect the opinions or views of the Los Alamos Scientific Laboratory.


Printed in USA. Price $3.00. Available from the Clearinghouse for Federal Scientific and Technical Information, National Bureau of Standards, United States Department of Commerce, Springfield, Virginia

LA-3415
UC-34, PHYSICS
TID-4500 (45th Ed.)

LOS ALAMOS SCIENTIFIC LABORATORY
of the
University of California

LOS ALAMOS • NEW MEXICO

Report written: August 1965

Report distributed: November 17, 1965

# Computation of Fast Neutron Penetration in Air by the "Sn-Method" with Special Emphasis on the Use of "Multitable-Multigroup Cross Section Sets"

by

H. A. Sandmeier
G. E. Hansen
R. B. Lazarus
R. J. Howerton*


*Lawrence Radiation Laboratory.



ABSTRACT

Much theoretical work has been done in the past to represent the angular dependence in the scattering source term of the Boltzmann equation by means of Legendre or other series expansions. However, relatively little work has been done to feed this information into our present day Sn codes. The Sn-transport codes at LASL allow a representation of anisotropy in the scattering-source term by means of multitable cross section sets, and we develop here a formalism to generate these sets. The numerical evaluation of Sn cross section entries for these multitable sets has been computerized by one of us (R.B.L.).

Deep penetration calculations (3000 meters) of high energy neutrons in homogeneous air are presented. These calculations used recently evaluated basic cross section data for nitrogen and oxygen from the LRL-LASL Library (Howerton tape).

The variations in the neutron flux due to different approximations are discussed as are also the expected variations in the flux due to inaccuracies in cross section data.

ACKNOWLEDGMENTS

We would like to thank our LASL colleagues, G. Bell, W. Goad, and K. Lathrop, and E. Plechaty of LRL for their help in this investigation.

CONTENTS



TABLES

TABLES (Continued)



ILLUSTRATIONS

# I. INTRODUCTION

The effect of anisotropic elastic scattering upon deep penetration of high energy neutrons in homogeneous air is examined. At large distances (3 - 4 km) considerable discrepancies have been observed in Monte Carlo calculations of the biological prompt-neutron dose due to a monoenergetic 14 MeV point source. Monte Carlo calculations allow an exact representation of the measured anisotropies but suffer from poor statistics at large distances.

Sn-transport codes at LASL allow the insertion of multitable cross section sets to represent anisotropies in the source term of the Boltzmann equation. Much theoretical work has been done in the past to represent the angular dependence in the source term by means of Legendre and other series expansions.

However, relatively little work has been done to feed this information into our present day Sn codes. This anisotropy representation requires multitable cross section sets. Provided that the computer memory is large enough to carry a sufficient number of space points to insure a good convergence on the flux and provided that a sufficient number of cross section tables to represent the scattering an-

isotropies is available, we should expect good results from an Sn-calculation. It is the purpose of this paper to present a consistent formalism to generate these multitable-multigroup cross section sets.

The solution of the Boltzmann transport equation by means of Legendre series expansion of both the flux and the anisotropic scattering source term is the most convenient link with multigroup Sn solutions. For plane geometry, the time independent Boltzmann transport equation is shown in Eqn. I-1.

$$\frac{\partial}{\partial z}\left\{\frac{(m+1)\Phi_{m+1,g}(z)+m\Phi_{m-1,g}(z)}{2m+1}\right\}+\Sigma_g(m)\Phi_{m,g}(z)=\sum_{g'}\Sigma_{m,g'\to g}(m)\Phi_{m,g'}(z)$$

$$m=0,1,2.....\qquad \text{EQN I-1}$$

where

$$\Phi_{m,g}(z)=\int_g \Phi_m(e,z)dE$$

$$\text{where}\quad \Phi_m(E,z)=\int_{-1}^{+1}\Phi(E,\mu,z)P_m(\mu)d\mu$$

$$\Sigma_g(m)=\int_g \Phi_m(E,z)\Sigma(E)dE \Big/ \int_g \Phi_m(E,z)dE$$

$$\Sigma_{n,g'\to g}(m)=\int_{g'} dE' \int_g dE\Phi_m(E',z)\Sigma_n(E'\to E) \Big/ \int_{g'} \Phi_m(E',z)dE'$$

$$\text{where}\quad \Sigma_n(E'\to E)=\int_{-1}^{+1}\Sigma(E'\to E,\mu)P_n(\mu)d\mu$$

On the other hand, the mathematical form of the multigroup-multitable equation solved in the Sn codes is

$$\mu \frac{\partial \Phi_g(\mu,z)}{\partial z} + \Sigma_g \Phi_g(\mu,z) = \sum_{g'} \Sigma^{(1)}_{g'\to g} P_o(\mu)\Phi_{o,g'}(z) +$$

$$+ \sum_{g'} \Sigma^{(2)}_{g'\to g} P_1(\mu)\Phi_{1,g'}(z) + \ldots + \sum_{g'} \Sigma^{(k)}_{g'\to g} P_{k-1}(\mu)\Phi_{k-1,g'}(z)$$

EQN I-2

We note that there is only <u>one</u> collision cross section $\Sigma_g$ in Eqn. I-2 as opposed to an infinite number of $\Sigma_g(m)$ in Eqn. I-1. Here the variable (m) indicates that each collision cross section is averaged with a different Legendre spectral component $\Phi_m(E,z)$. The superscripts (1), (2) ..... (k) for the transfer coefficients in Eqn. I-2 characterize the order of scattering anisotropy. Therefore, if we truncate the RHS of Eqn. I-2 at k = 2, we need two tables of cross sections; for k = 3 we need 3 tables; etc.

Since the mathematical form of Eqn. I-2 is different from Eqn. I-1, we are confronted with the problem of choosing values for the collision cross section $\Sigma_g$ and the transfer coefficients $\Sigma^{(1)}_{g'\to g}$, $\Sigma^{(2)}_{g'\to g}$ ..... $\Sigma^{(k)}_{g'\to g}$ so as to make the solution of these two equations as nearly equivalent as possible. These numerical quantities are the only information we are able to furnish to the Sn machine calculation. In the following we describe two recipes for obtaining the k-table cross sections appearing in Eqn. I-2 as well as two special cases.

## II. THEORY

The general time independent Boltzmann transport equation is

$$\vec{\Omega}\cdot\nabla_{\vec{r}}\,\Phi(E,\vec{\Omega},\vec{r}) + \Sigma(E)\Phi(E,\vec{\Omega},\vec{r}) = \int_{E'}\int_{\vec{\Omega}'}\Phi(E',\vec{\Omega}',\vec{r})\Sigma(E'\to E,\vec{\Omega}'\to\vec{\Omega})dE'd\vec{\Omega}' + S(E,\vec{\Omega},\vec{r}) \qquad \text{EQN II-1}$$

Equation II-1 states that the total derivative of the time independent flux $\Phi(E,\vec{\Omega},\vec{r})$ in the direction $\vec{\Omega}$ equals the rate at which neutrons are introduced (in that direction) represented by the RHS of Eqn. II-1, less the rate of removal (2nd term LHS) by collision.

The RHS of Eqn. II-1 contains two source terms, the first or homogeneous term being a linear function of the flux and the second or inhomogeneous term $S(E,\vec{\Omega},\vec{r})$ being independent of the flux. In neutron penetration problems, the homogeneous term $\int_{E'}\int_{\vec{\Omega}'}\Phi(E',\vec{\Omega}',\vec{r})\Sigma(E'\to E,\vec{\Omega}'\to\vec{\Omega})dE'd\vec{\Omega}'$ can be decomposed into contributions from (a) elastic scattering (n,n); (b) inelastic scattering (n,n'), (n,2n), etc.; and (c) fission. The generalized macroscopic differential scattering cross section $\Sigma(E'\to E,\vec{\Omega}'\to\vec{\Omega})$, therefore, includes all productive events such as (n,n'), (n,2n) fission, etc. This cross section depends on energy E and direction $\vec{\Omega}$ of the

"emitted" neutrons as well as on E' and $\vec{\Omega}'$ of the "incident" neutrons.

For simplicity, we reduce the variables in the flux to correspond to one-dimensional slab geometry

$$\Phi(E,\vec{\Omega},\vec{r}) \Rightarrow \Phi(E,\mu,z) \qquad \text{EQN II-2}$$

Here $\mu = \vec{\Omega}\cdot\hat{z}$ (i.e. cosine of the angle between the neutron direction $\vec{\Omega}$ and the $\hat{z}$-axis). For this we have to make two assumptions. The first is the plane geometry assumption with variable z and secondly, the scattering assumption expressed in Eqn. II-3.

$$\Sigma(E'\rightarrow E,\vec{\Omega}'\rightarrow\vec{\Omega}) = \Sigma(E'\rightarrow E,\vec{\Omega}'\cdot\vec{\Omega}) \equiv \Sigma(E'\rightarrow E,\mu_o) \qquad \text{EQN II-3}$$

Here $\mu_o = \vec{\Omega}'\cdot\vec{\Omega}$ the cosine of the scattering angle, that is, the angle between the incident and scattered or emitted neutron direction. Physically this is true for materials in which the scattering does not depend on the incident direction. For crystalline materials with a distinct layer structure, this assumption would, however, not be valid at low neutron energies.

The cosine of the scattering angle $\mu_o$ in II-3 is a function of four variables, i.e. $\mu'$ and $\mu$ and the azimuthal angles $\varphi'$ and $\varphi$.

$$\mu_o = \mu\mu' + \sqrt{1-\mu'^2}\ \sqrt{1-\mu^2}\ \cos(\varphi-\varphi') \qquad \text{EQN II-4}$$

We now expand $\Sigma(E'\rightarrow E,\mu_o)$ into spherical harmonics

$$\Sigma(E'\rightarrow E,\mu_o) = \sum_{n=0}^{\infty} \frac{2n+1}{4\pi}\,\Sigma_n(E'\rightarrow E)P_n(\mu_o) \qquad \text{EQN II-5}$$

where

$$\Sigma_n(E' \rightarrow E) = 2\pi \int_{-1}^{+1} \Sigma(E' \rightarrow E, \mu_o) P_n(\mu_o) d\mu_o \qquad \text{EQN II-6}$$

To permit the integration of the homogeneous source term in Eqn. II-1, we must express Eqn. II-5 as $f(\mu', \mu, \varphi', \varphi)$ by using the addition theorem for Legendre polynomials.

$$P_n(\mu_o) = P_n(\mu) P_n(\mu') + 2 \sum_{m=1}^{n} \frac{(n-m)!}{(n+m)!} P_n^{(m)}(\mu) P_n^{(m)}(\mu') \cos m(\varphi - \varphi') \qquad \text{EQN II-7}$$

In Eqn. II-1 we have to integrate the homogeneous source term over $d\Omega' = d\mu' d\varphi'$. By integrating Eqn. II-7 over $\varphi'$ we note that the cosine term will become zero. Therefore,

$$\int_0^{2\pi} P_n(\mu_o) d\varphi' = 2\pi P_n(\mu) P_n(\mu') + 0 \qquad \text{EQN II-8}$$

We now insert Eqn. II-5 into Eqn. II-1 and integrate over $d\varphi'$ to obtain

$$\mu \frac{\partial \Phi(E,\mu,z)}{\partial z} + \Sigma(E)\Phi(E,\mu,z) = \sum_{n=0}^{\infty} \frac{2n+1}{2} P_n(\mu) \int_{E'} dE' \int_{-1}^{+1} \Phi(E',\mu',z) \times$$

$$\times \Sigma_n(E' \rightarrow E) P_n(\mu') d\mu' + S(E,\mu,z) \qquad \text{EQN II-9}$$

The first term on the LHS of Eqn. II-1 becomes $\mu \frac{\partial \Phi(E,\mu,z)}{\partial z}$ in Eqn. II-9

since $\mu$ is the cosine of the angle between the neutron direction $\vec{\Omega}$ and the vector in the z-direction. In Eqn. II-9 we have assumed that we can represent the inhomogeneous source $S(E,\mu,z)$ in the same way as the homogeneous source. Consistent with the expansion of the scattering source, Eqns.II-5 and II-6, we now expand the flux also in a series of polynomials

$$\Phi(E',\mu',z) = \sum_{n=0}^{\infty} \frac{2n+1}{4\pi} P_n(\mu')\Phi_n(E',z) \qquad \text{EQN II-10}$$

with

$$\Phi_n(E',z) = 2\pi \int_{-1}^{+1} \Phi(E',\mu',z)P_n(\mu')du' \qquad \text{EQN II-11}$$

Similarly we could write the inhomogeneous source term as

$$S(E,\mu,z) = \sum_{n=0}^{\infty} \frac{2n+1}{4\pi} P_n(\mu)\ S_n(E,z) \qquad \text{EQN II-12}$$

where

$$S_n(E,z) = 2\pi \int_{-1}^{+1} S(E,\mu,z)P_n(\mu)d\mu \qquad \text{EQN II-13}$$

Since the inhomogeneous source term plays no role in the multitable-multigroup cross section representation, we shall however no longer carry this term explicitly.

Insert Eqn. II-11 into Eqn. II-9

$$\mu \frac{\partial \Phi(E,\mu,z)}{\partial z} + \Sigma(E)\Phi(E,\mu,z) = \sum_{n=0}^{\infty} \frac{2n+1}{2} P_n(\mu) \int_{E'} dE' \Sigma_n(E' \rightarrow E)\Phi_n(E',z)$$

EQN II-14

Multiply Eqn. II-14 by $P_m(\mu)$ and integrate over $\mu$

$$\frac{\partial}{\partial z} \int_{-1}^{+1} \mu P_m(\mu)\Phi(E,\mu,z)d\mu + \Sigma(E)\Phi_m(E,z) =$$

$$= \sum_{n=0}^{\infty} \frac{2n+1}{2} \int_{-1}^{+1} P_n(\mu)P_m(\mu)d\mu \int_{E'} \Sigma_n(E' \rightarrow E)\Phi_n(E',z)dE' \quad \text{EQN II-15}$$

Finally, using

$$\mu P_m(\mu) = \frac{(m+1)P_{m+1}(\mu) + mP_{m-1}(\mu)}{2m+1} \quad \text{EQN II-16}$$

and

$$\int_{-1}^{+1} P_n(\mu)P_m(\mu)d\mu = \frac{2}{2m+1} \delta_{mn} \quad \text{EQN II-17}$$

we arrive at the standard polynomial representation of the transport equation

$$\frac{\partial}{\partial z}\left\{\frac{(m+1)\Phi_{m+1}(E,z)+m\Phi_{m-1}(E,z)}{2m+1}\right\} + \Sigma(E)\Phi_m(E,z) = \int_{E'}\Sigma_m(E'\to E)\Phi_m(E',z)dE'$$

$$m = 0,1,2.....$$

where $$\Phi_m(E,z) = \int_{-1}^{+1}\Phi(E,\mu,z)P_m(\mu)d\mu$$

$$\Sigma_m(E'\to E) = \int_{-1}^{+1}\Sigma(E'\to E,\mu_o)P_m(\mu_o)d\mu_o \qquad \text{EQN II-18}$$

Explicitly,

(m = 0)

$$\frac{\partial}{\partial z}\Phi_1(z) + \Sigma(E)\Phi_o(z) = \int_{E'}\Sigma_o(E'\to E)\Phi_o(E',z)dE'$$

(m = 1)

$$\frac{\partial}{\partial z}\left\{\frac{2\Phi_2(E,z)+\Phi_o(E,z)}{3}\right\} + \Sigma(E)\Phi_1(E,z) = \int_{E'}\Sigma_1(E'\to E)\Phi_1(E',z)dE'$$

(m = 2)

$$\frac{\partial}{\partial z}\left\{\frac{3\Phi_3(E,z)+2\Phi_1(E,z)}{5}\right\}+\Sigma(E)\Phi_2(E,z)=\int_{E'}\Sigma_2(E'\to E)\Phi_2(E',z)dE'$$

$$\vdots \qquad\qquad \vdots \qquad\qquad \vdots$$

We now introduce a multigroup notation, i.e. subdivide the energy range into groups and integrate Eqn. II-18 over the g group energy interval.

$$\frac{\partial}{\partial z}\left\{\frac{(m+1)\Phi_{m+1,g}(z)+m\Phi_{m-1,g}(z)}{2m+1}\right\}+\Sigma_g(m)\Phi_{m,g}(z)=\sum_{g'}\Sigma_{m,g'\to g}(m)\Phi_{m,g'}(z)$$

$$m = 0,1,2.....$$

where $\Phi_{m,g}=\int_g\Phi_m(E,z)dE$

$$\Sigma_g(m)=\int_g\Phi_m(E,z)\Sigma(E)dE\Big/\int_g\Phi_m(E,z)dE$$

$$E_{n,g'\to g}(m)=\int_{g'}dE'\int_g dE\Phi_m(E',z)\Sigma_n(E'\to E\Big/\int_{g'}\Phi_m(E',z)dE'$$

EQN II-19

Eqn. II-19 is, of course, still an exact representation of Eqn. II-1, the original Boltzmann transport equation. The index (m) in $\Sigma_g(m)$ and $\Sigma_{n,g'\to g}(m)$ in Eqn. II-19 refers to the order of the flux $\Phi_m(E,z)$ used in the cross section averaging scheme.

The mathematical form of the multigroup-multitable transport equation solved in Sn codes is

$$\mu \frac{\partial \Phi_g(\mu,z)}{\partial z} + \Sigma_g \Phi_g(\mu,z) = \sum_{g'} \Sigma^{(1)}_{g'\to g} P_o(\mu)\Phi_{o,g'} + \sum_{g'} \Sigma^{(2)}_{g'\to g} P_1(\mu)\Phi_{1,g'} +$$

$$+ \ldots\ldots + \sum_{g'} \Sigma^{(k)}_{g'\to g} P_{k-1}(\mu)\Phi_{k-1,g'}(z)$$

EQN II-20

The superscripts (1) (2).....(k) for the transfer coefficients in Eqn. II-20 characterize the order of scattering anisotropy. Therefore, if we truncate the RHS of Eqn. II-20 at k = 2 we need two tables of cross sections; for k = 3 we need three tables; etc.

The expansion of Eqn. II-20 in Legendre polynomials gives a set of equations somewhat different from Eqn. II-19; namely,

$$\frac{\partial}{\partial z}\left\{\frac{(m+1)\Phi_{m+1,g}+m\Phi_{m-1,g}}{2m+1}\right\} + \Sigma_g \Phi_{m,g} = \sum_{g'} \Sigma^{(m+1)}_{g'\to g}\Phi_{m,g};\quad m = 0,1,2\ldots,k-1$$

$$\frac{\partial}{\partial z}\left\{\frac{(m+1)\Phi_{m+1,g}+m\Phi_{m-1,g}}{2m+1}\right\} + \Sigma_g \Phi_{m,g} = 0; \qquad m = k,k+1,\ldots..$$

EQN II-20a

We note that there is only <u>one</u> collision cross section $\Sigma_g$ in Eqn. II-20a as opposed to an infinite number of $\Sigma_g(m)$ in Eqn. II-19.

Since the mathematical form of Eqn. II-20a is different from Eqn. II-19, we are confronted with the problem of choosing values for the collision cross section $\Sigma_g$ and the transfer coefficients $\Sigma^{(1)}_{g'\to g}$, $\Sigma^{(2)}_{g'\to g}$ $\ldots\ldots\Sigma^{(k)}_{g'\to g}$ so as to make the solution of these two equations as nearly equivalent as possible. These numerical quantities are the only information we are able to furnish to the Sn machine calculation. In the following we describe two recipes for obtaining the k-table cross sections appearing in Eqn. II-20.

## THE k-TABLE "CONSISTENT $P_{k-1}$" RECIPE

By adding $\left[\Sigma_g(o)-\Sigma_g(m)\right]\Phi_{m,g}(z)$ to both sides of Eqn. II-19 we obtain formal agreement with Eqn. II-20a for $m = 0,1,2....k-1$ under the identifications

$$\Sigma_g = \Sigma_g(o)$$

$$\Sigma_{g'\to g}^{(m+1)} = \Sigma_{m,g'\to g}(m) + \left[\Sigma_g(o)-\Sigma_g(m)\right]\delta_{g'g} \qquad \text{EQN II-21}$$

The first error in this identification appears at $m = k$, and depends on the magnitude of

$$\sum_{g'} \Sigma_{k,g'\to g}(k)\Phi_{k,g'}(z) + \left[\Sigma_g(o)-\Sigma_g(k)\right]\Phi_{k,g}$$

To the extent that the $k^{th}$ harmonic component of the flux is small, the identification of Eqn. II-21 is good.

Note that the identification in Eqn. II-21 is not unique: one could have, with the same precision, identified $\Sigma_g$ with any $\Sigma_g(m')$ for $m' \leq k-1$, as may be verified by the above artifice of adding $\left[\Sigma_g(m')-\Sigma_g(m)\right]\Phi_{m,g}$ to both sides of Eqn. II-19. Our choice of $m' = 0$ has the advantage that the value of the collision cross section $\Sigma_g$ is independent of the number of tables k.

THE "k-TABLE" TRANSPORT RECIPE

Here one approximates the generalized scattering cross section as

$$\Sigma(E'\to E,\mu) \simeq \sum_{n=o}^{k-1} \Sigma_n(E'\to E)P_n(\mu)+\Sigma_k(E')\delta(E'\to E)P_k(\mu) \qquad \text{EQN II-22}$$

where

$$E_k(E') = \int_E \int_{-1}^{+1} \Sigma(E'\to E,\mu)P_k(\mu)d\mu dE$$

and thereby reduces Eqn. II-19 to

$$\frac{\partial}{\partial z}\left\{\frac{(m+1)\Phi_{m+1,g}(z)+m\Phi_{m-1,g}(z)}{2m+1}\right\} + \Sigma_g(m)\Phi_{m,g}(z) = \sum_{g'} \Sigma_{m,g'\to g}(m)\Phi_{m,g'}(z)$$

$$m = 0,1,2.....(k-1)$$

$$\frac{\partial}{\partial z}\left\{\frac{(k+1)\Phi_{k+1,g}(z)+k\Phi_{k-1,g}(z)}{2k+1}\right\} + \Sigma_g(k)\Phi_{k,g}(z) = \Sigma_{k,g}(k)\Phi_{k,g}(z)$$

$$\frac{\partial}{\partial z}\left\{\frac{(m+1)\Phi_{m+1,g}(z)+m\Phi_{m-1,g}(z)}{2m+1}\right\} + \Sigma_g(m)\Phi_{m,g}(z) = 0$$

$$m = k+1, k+2, .....$$

EQN II-19a

Now, by adding $\left[\Sigma_g(k)-\Sigma_{k,g}(k)-\Sigma_g(m)\right]\Phi_{m,g}$ to both sides of Eqns. II-19a,

we again obtain formal agreement with Eqns. II-20a for $m = 0,1,2....(k-1)$ under the identifications

$$\Sigma_g = \Sigma_g(k) - \Sigma_{k,g}(k)$$

$$\Sigma_{g' \to g}^{(m+1)} \equiv \Sigma_{m,g' \to g}(m) + \left[\Sigma_g(k) - \Sigma_{k,g}(k) - \Sigma_g(m)\right]\delta g'g \qquad \text{EQN II-23}$$

The first error in this identification again appears at $m = k$, and depends on the magnitude of

$$\Sigma_{k,g}(k)\Phi_{k,g}(z) - \sum_{g'} \Sigma_{k,g' \to g}(k)\Phi_{k,g'}(z)$$

This error can be small even though the magnitude of the $k^{th}$ harmonic component of the flux is not. For example, when anisotropy is associated purely with heavy element elastic scattering, $\Sigma_{k,g' \to g}(k) \cong 0$ for $g' \neq g$ (i.e. trivial energy loss in the anisotropic scattering processes) and $\Sigma_{k,g}(k) \simeq \Sigma_{k,g \to g}(k)$.

One point of clarification may be made here regarding both recipes. In a practical problem we don't know the spectra $\Phi_o(E,z), \Phi_1(E,z), \Phi_2(E,z)$, etc., which after all are the quantities we want to calculate. We are, however, forced to make assumptions as to how these spectra will look in order to evaluate the above group cross sections. One could, of course, follow an iterative procedure by making a guess for the expected spectrum and then computing the group cross sections and thence a first

iterative spectrum. But, what is needed for averaging is a fine scale spectrum within a group,and what is given by calculation is a coarse group-wise spectrum. An estimate of such fine scale spectra may not be too difficult save perhaps in resonance regions.

For infinite homogeneous media, the energy spectra of various harmonic components of the flux are related by $\Phi_m(E) \sim \frac{\Phi_{m-1}(E)}{\Sigma(E)-\Sigma_m(E)}$ ; a simple approximation to this is $\Phi_m(E) \sim \Phi_o(E)[\Sigma_{tr}(E)]^{-m}$.

## III. CALCULATION OF GROUP-AVERAGED CROSS SECTIONS

The various group-averaged cross sections defined in the preceding chapters were calculated for nitrogen and oxygen from nuclear data tabulated in the format of R. Howerton's magnetic tape library of evaluated nuclear data. Almost without exception, Howerton's data were used. These data are of three types:

1. Cross Sections. A sequence of $(E,\Sigma)$ pairs for each reaction, spaced sufficiently closely in energy so that we may assume $\Sigma(E) = \alpha E^b$ between pairs (piece-wise linear on a log-log basis).

2. Angular Distributions. For a variety of incident neutron energies, $E'$, a sequence of $(T,\mu')$ pairs giving the angular distribution of elastic scattering in the center of mass system as a piece-wise function normalized to

$$\int_{-1}^{+1} T(\mu',E')d\mu' = 1 \qquad \text{III-1}$$

It was assumed that $T(\mu',E')$ was piece-wise linear in $1/E'$. Nonelastic reactions were assumed to be isotropic.

3. For each nonelastic, nonabsorbing reaction, for a variety

of incident neutron energies, E', a sequence of (N,E) pairs giving the number of secondaries per MeV coming out with energy E, per incident neutron as a piece-wise linear function normalized to

$$\int_0^\infty N(E',E)dE = \text{number of secondaries}$$

The elastic angular distributions were preprocessed to form the array of numbers

$$F_{n,t,j} = \int_{-1}^{\mu'_t} d\mu' T(\mu',E'_j)P_n(\mu) \qquad \text{III-2}$$

where

$$\mu = \frac{1 + A\mu'}{\sqrt{(1 + A^2 + 2A\mu')}} \qquad \text{III-3}$$

is the laboratory system cosine corresponding to the center of mass cosine, $\mu'$. A is the mass of the scatterer in units of the neutron mass. $P_n$ is the $n^{th}$ Legendre polynomial. j labels the incident energies for which data were given, with $E'_j > E'_{j-1}$. $\mu'_t = -1 + 2t/T$, for $t = 0,1,\cdots T$; $T = 100$ was used. The integrals were evaluated by Simpson's Rule with a step size of $1/T$. The quantities

$$F_{n,t}(E') = \int_{-1}^{\mu'_t} d\mu' T(\mu',E')P_n(\mu) \qquad \text{III-4}$$

were then found by double linear interpolation on $\mu'$ and $1/E'$. An integral $\int_{\mu'_1}^{\mu'_2} d\mu'$ was replaced by $\int_{-1}^{\mu'_2} d\mu' - \int_{-1}^{\mu'_1} d\mu'$. Note that $F_{0,T,j} = 1$ and $F_{1,T,j} = \bar{\mu}(E'_j)$.

The secondary energy data were preprocessed to form the array of numbers

$$N^r_{j\to g} = \int_g dE\, N^r(E'_j \to E) \qquad \text{III-5}$$

where r labels reactions (n,n'), (n,2n), etc. The numbers

$$N^r_g(E^*) = \int_g dE N^r(E^* \to E) \qquad \text{III-6}$$

In principle, as estimate of the flux $\Phi(E,\mu)$ should come from some previous approximate solution of the problem of interest, or of some similar problem. From this function, one would first calculate the functions

$$\Phi_m(E) = \int_{-1}^{1} d\mu \Phi(E\mu) P_m(\mu), \quad m = 0,1,2,\cdots \qquad \text{III-7}$$

For a given set of energy groups, these functions may be replaced by the normalized, piece-wise-discontinuous functions

$$\phi_m^*(E) \equiv \Phi_m(E) \int_g dE' \Phi_m(E') \qquad \text{III-8}$$

where the integration is over that energy group which embraces E. Note that, because of the normalization,

$$\int_g dE \Phi_m^*(E) \equiv 1 \qquad \text{III-9}$$

only the relative energy dependence of the weight functions $\Phi_m^*(E)$ within each group is of importance.

In practice, Eq. III-7 was not used. Instead, we used the approximate relation

$$\Phi_m(E) \approx \Phi_{m-1}(E)/\sigma_{tr}(E) \qquad \text{III-10}$$

suggested by Gordon Hansen. It is planned in the near future to investigate the effects of this approximation. By $\sigma_{tr}(E)$ is meant $\sigma_{total}(E) - \bar{\mu}(E)\sigma_{elastic}(E)$. This relation was used, then, with only the flux distribution, $\Phi_0(E)$, specified ad hoc.

Let us consider now the collision cross sections

$$\sum_{n,g}(m) = \int_g dE\, \phi_m^*(E) \Sigma_n(E) \qquad \text{III-11}$$

where

$$\Sigma_n = \int_{-1}^{1} d\mu' \Sigma(\mu') P_n(\mu) \qquad \text{III-12}$$

and the transfer coefficients

$$\sum_{n,g'\to g}(m) = \int_g dE \int_{g'} dE' \Sigma_n(E'\to E)\phi_m^*(E') \qquad \text{III-13}$$

Note that $\Sigma(E'\to E)$ is a neutron <u>production</u> cross section; thus, for example,

$$\int_0^\infty dE \Sigma^{n,2n}(E'\to E) = 2\Sigma^{n,2n}(E') \qquad \text{III-14}$$

The nonelastic contributions to these quantities vanish for $m \neq 0$, leaving

$$\sum_{o,g}^{nonel.}(m) = \int_g dE \phi_m^*(E)\, \Sigma^{nonel.}(E)$$

$$\sum_{0,g'\to g}^{nonel.}(m) = \int_{g'} dE' \phi_m^*(E') \sum_{nonel.} \Sigma^r(E') N_g^r(E') \qquad \text{III-15}$$

The elastic contribution to the collision cross section is

$$\sum_{n,g}^{el.}(m) = \int_g dE \phi_m^*(E) \Sigma^{el}(E) F_{n,T}(E) \qquad \text{III-16}$$

The elastic contribution to the transfer coefficients is

$$\sum_{n,g'\to g}^{el}(m) = \int_{g'} dE'\Phi_m^*(E')\Sigma^{el}(E')F_n^g(E',\Delta\mu') \qquad \text{III-17}$$

where

$$F_n^g(E',\Delta\mu') = \int_{\Delta\mu'(E',g)} d\mu' T(\mu')P_n(\mu) \qquad \text{III-18}$$

and $\Delta\mu'(E',g)$ spans the angular interval within which an incoming neutron of lab energy E' scatters elastically into a lab energy, E, which lies within group g. Specifically, the integral is from $\mu'_{min}$ to $\mu'_{max}$, where

$$\mu'_{min} = \max\left\{-1, \left[(1+A)^2 E_{min_g} - (1+A^2)E'\right]\Big/2AE'\right\}$$

$$\mu'_{max} = \min\left\{+1, \left[(1+A)^2 E_{max_g} - (1+A^2)E'\right]\Big/2AE'\right\} \qquad \text{III-19}$$

$F_n^g(E',\Delta\mu')$ is taken as zero if $\Delta\mu'(E',g)$ is negative.

The integration formula used for the energy integrals was that for sums and products of functions of the form $f(E) = \alpha E^b$. The cross sections (including the calculated $\sigma_{tr}$) and the flux, $\Phi_0$, were assumed to be of this form between data points. Because $F_n^g(E',\Delta\mu')$ has no simple energy dependence, the integration steps $E'_1$ to $E'_2$ were kept small, for the elastic case, as long as the scattering out of group was non-zero.

## IV. MICROSCOPIC CROSS SECTIONS

The cross sections, and associated nuclear data, used in these calculations are those of the IRL-LASL neutron data tape library.

It is the objective of this section to present the data for nitrogen and oxygen with a short description (for each energetically possible reaction) of the methods used in deriving the cross section values.

Since there are large energy ranges and a number of energetically possible reactions which have never been measured, the library is regarded, always, as being a current approximation. As new experimental data become available, they are compared with the values on tape; and changes in the library are made where necessary.

Cross sections and other data are presented in a form suitable for linear-linear interpolation. All angular distributions and energy distributions of secondaries are presented in a normalized form, such that the integral over the cosine of the angle or over secondary energy is unity.

## NITROGEN

IV-1. The following reactions have thresholds below 15 MeV.

| Reaction | Threshold (MeV) |
|---|---|
| n,γ | 0. |
| n,p | 0. |
| n,α | .16 |
| n,n'γ | 2.47 |
| n,t | 4.29 |
| n,d | 5.70 |
| n,n'p | 8.09 |
| n,n'd | 11.00 |
| n,2n | 11.31 |
| n,n'α | 12.43 |

IV-2. Total Cross Section

From .025 eV to .001 MeV the values are taken from Reference 1.* From .001 MeV to .08 MeV, a smooth variance is assumed to connect the measurements above and below this range. From .08 to .85 MeV the values are based on the measurements of Reference 2, and from .85 to 2.1 MeV they are based on Reference 3. For the remainder of the energy range, i.e., from 2.1 to 14.6 MeV, the data of Reference 4 are used as the basis of the total cross sections.

---

*References for Chapter IV are on page 40.

IV-3. n,γ Cross Section

At .025 eV the value recommended in Reference 5 is used. It is assumed that the cross section drops generally as 1/v to 1 mb at 100 eV, then to zero at 300 eV and above.

IV-4. n,p Cross Section

From a mean of measured values, taken to be 1.78 b at .025 eV, the cross section is assumed to fall as 1/v to a minimum of 1.5 mb at 100 KeV. From this minimum it follows in accordance with References 6 and 7 to about 4.1 MeV. From a value of 84 mb at 4.1 MeV to 14.6 MeV, there are no measurements, so the cross section is assumed to fall to 25 mb at 4.75 MeV and then to 15 mb at 14.6 MeV. There is probably resonance structure in this energy range, but with no measurements it is assumed that the cross section will fall on the average because of competing reactions.

IV-5. n,α Cross Section

The threshold of this reaction is at .16 MeV. It does not rise to a value of 10 mb until about 1.3 MeV. From about 1.4 to 5.0 MeV the cross section was measured, as reported in Reference 7. From about 5 MeV to 8.5 MeV the measurement included the n,t reaction as well as the n,α reaction. For a limited range (5.75 to 8.25 MeV) the n,t reaction was differentiated and reported. It was about an order of magnitude lower than the n,α reaction. The n,t reaction was lumped with the

n,α reaction because of the restricted range for which n,t was measured and its low value. From 8.5 MeV to 14.6 MeV there is only one measurement, Reference 8, at about 14 MeV, done with a cloud chamber. This measurement was for alpha emission so any n,n'α would be included. With the uncertainty associated with this measurement, it was decided to straight-line the cross section from a value of 100 mb at 8.5 MeV to 40 mb at 14.6 MeV.

IV-6. n,n'γ Cross Section

The measurements of Reference 9 define the cross section to about 8.0 MeV. At 14.1 MeV a measurement (Reference 10) of nonelastic neutron emission defines the cross section for the sum of 2(n,2n) + n,n'γ + n,n'p + n,n'd + n,n'α reactions. Since the only one of these reactions which has been measured at 14 MeV is the n,2n reaction, the others are lumped together and called the n,n'γ reaction, for convenience. The value at 8.0 MeV is connected smoothly to the value at 14.1 MeV.

IV-7. n,t Cross Section

The n,t cross section is lumped with the n,α cross section as described above.

IV-8. n,d Cross Section

This reaction has not been measured. It is felt from systematics

that it is probably of the order of 10 to 20 mb; and, consequently, little is lost by ignoring it, as has been done here.

IV-9. n,n'p; n,n'd; n,n'α Cross Sections

These reactions have not been measured and consequently are lumped with the n,n'γ as described above.

IV-10. n,2n Cross Section

In most recent data, Reference 5, a value of 8 mb at 14.6 MeV is reported. We have used an older value of 5.1 mb, but the difference is within the uncertainty of the total nonelastic.

IV-11. Elastic Cross Section

In general, this cross section was derived by subtracting the nonelastic cross section from the total with the results checked against the integrated elastic reported in Reference 5. In two cases these did not agree. Both times, the difficulty was resolved in favor of the subtractive process.

IV-12. Elastic Angular Distributions

These are presented in normalized form such that the integral of the angular distribution is unity. The data, from which the angular distributions are derived, are those presented in Reference 11.

IV-13. n,n'γ and n,2n Angular Distributions

These are assumed isotropic in the center of mass system.

IV-14. n,n'γ and n,2n Energy Distributions for Secondaries

At 14.0 MeV these are derived from Reference 10. Below 14.0 MeV, the values are guessed, taking into account appropriate level schemes.

## OXYGEN

IV-15. The following reactions have thresholds below 15 MeV.

| Reaction | Threshold (MeV) |
|---|---|
| n,γ | 0. |
| n,α | 2.35 |
| n,n'γ | 6.43 |
| n,n'α | 7.60 |
| n,p | 10.22 |
| n,d | 10.51 |
| n,n'p | 12.88 |

IV-16. Total Cross Section

The total cross section is essentially the same as that presented in References 1 and 5. Below one KeV the values of Reference 1 were used. Between 1 KeV and 14.6 MeV the data points in the IRL tape library of experimental cross sections were plotted mechanically and a curve drawn, from which points were chosen for this presentation. The references from which the experimental points were taken are the same as those of References 1 and 5.

IV-17. n,γ Cross Section

This cross section is less than 0.2 mb at .025 eV and was ignored for the purpose of these calculations since it may be assumed to be non-

rising with increasing energy.

IV-18. n,$\alpha$ Cross Section

This cross section is measured to be not greater than 4 mb at 3.65 MeV (Reference 12). It is therefore assumed to have an effective threshold at 3.6 MeV. From 2.6 to 9.0 MeV, the data of References 12, 13, 14 are used. From 9.0 to 14.6 MeV the cross section is assumed constant at 80 mb. Although there are surely resonances in this region, there have been no measurements; and the 80 mb value is a hopeful attempt to present an average in this region.

IV-19. n,n'$\gamma$ Cross Section

The values used here generally follow the measurements of Reference 9, up to 9.5 MeV. From 9.5 to 14.6 MeV the values are interpolated smoothly to tie into the 500 mb value reported in Reference 15.

IV-20. n,n'$\alpha$ and n,n'p Cross Sections

These cross sections are assumed to be included in the n,n'$\gamma$ cross section. They have not been measured.

IV-21. n,p Cross Section

This cross section has been well measured, and the values used here are derived from the measurements reported in Reference 5.

IV-22. n,d Cross Section

This reaction has not been measured and is ignored here. It is possible that it could have a 10 to 20 mb cross section at 14.6 MeV, which would still be within the uncertainty of the total absorption cross section at this energy.

IV-23. Elastic Cross Section

This cross section is derived by subtraction of the sum of the nonelastic cross sections from the total.

IV-24. Elastic Angular Distributions

These are presented in normalized form such that the integral of the angular distribution is unity. The data from which the angular distributions are derived are those presented in Reference 11.

IV-25. n,n'$\gamma$ Angular Distribution

Assumed isotropic for lack of data.

IV-26. n,n'$\gamma$ Energy Distribution of Secondaries

These are derived from consideration of the $O^{16}$ level scheme.

## CHAPTER IV - REFERENCES


1. BNL-325 Second Edition (1958) D. J. Hughes, R. B. Schwartz.
2. Private Communication (1962) E. G. Bilpuch, J. A. Farrell, G. C. Kyker, Jr., F. B. Parks, H. Newson.
3. Phys. Rev. 86, 483 (1952) J. J. Hinchey, P. H. Stelson, W. M. Preston.
4. Private Communication (1964) D. G. Foster, Jr., D. W. Glasgow.
5. BNL-325 Second Edition, Supp. 2 (1964) J. R. Stehn, M. D. Goldberg, B. A. Magurno, R. Wiener-Chasman.
6. Phys. Rev. 80, 818 (1950) C. H. Johnson, H. H. Barschall.
7. Nuclear Phys. 14, 277 (1959)F. Gabbard, H. Bichsel, T. W. Bonner.
8. Phys. Rev. 87, 716 (1952) A. B. Lillie.
9. Nuclear Phys. 14 295 (1959/60) H. E. Hall, T. W. Bonner.
10. Private Communication (1964) John Anderson.
11. BNL-400, Second Edition, Vol. 1 (1962) M. D. Goldberg, V. M. May, J. R. Stehn.
12. Helv. Phys. Acta, 28, 227 (1955) J. Seitz, P. Huber.
13. Phys. Rev. 107, 1065 (1957) R. B. Walton, J. D. Clement, F. Boreli.
14. Nuclear Phys. 48, 169 (1963) E. A. Davis, T. W. Bonner, D. W. Worley, Jr., R. Bass.
15. Phys. Rev. 89, 712 (1953) J. P. Conner.

# V. NUMERICAL EVALUATION OF MULTIGROUP MULTITABLE MACROSCOPIC CROSS SECTION SETS FOR SEA LEVEL AIR

## Air Data

| | |
|---|---|
| 1.22 gram/liter | sea level air<br>normal day 15° C |
| nitrogen 79% | $4.024 \times 10^{-5} \times 10^{24}$ nuclei/cc |
| oxygen 21% | $1.070 \times 10^{-5} \times 10^{24}$ nuclei/cc |

Section V-1 of this chapter reviews briefly the way in which various partial cross sections contribute to the collision and generalized scattering cross sections. Section V-2 presents the k-table "consistent" $P_{k-1}$ recipe (Eqn. II-21) explicitly for 1-table consistent $P_0$ to 5-table consistent $P_4$, while Section V-3 gives the corresponding Sn cross section entries for the k-table "transport" recipe (Eqn. II-24). Section V-4 gives two additional recipes which have been used at Los Alamos, namely a "1-table weapons transport approximation" which sacrifices accuracy in neutron energy losses through anisotropic scattering in order to guarantee positive in-group scattering cross sections, and a "2-table $P_1$ approximation (Bell)" which uses flux weighting only.

Numerical values of the macroscopic cross sections of sea-level air in a 25-group structure, defined in Table V-1, are illustrated in Tables

V-2 through V-6 for the 1, 3, and 5-table transport recipes and for the 5-table consistent $P_4$ recipe. Although group absorption cross sections do not appear explicitly in the Sn entries, their values are implied by the $\Sigma_g$ and $\Sigma_{g' \to g}$ and should be the same for <u>all</u> multitable recipes. We have listed these implied group absorption cross sections as a convenient check of numerical consistency. One may note, in comparing say the $\Sigma_g$ values for 5-table transport vs 5-table consistent computations, that corresponding entries differ considerably. However, as will be seen later in Chapter VI, their net implications for neutron penetration in air are essentially identical.

## V-1 An Elaboration on the Cross Sections Entering the Transport Equation

The general time independent Boltzmann transport equation adapted to Sn notation is shown in Eqn. V-1.

$$[\vec{\Omega}\cdot\vec{\nabla} + \Sigma(E)]\Phi(E,\vec{\Omega}) = \int_{E'}\int_{\vec{\Omega}'}\Phi(E',\vec{\Omega}')\Sigma(E'\to E,\vec{\Omega}'\cdot\Omega)dE'd\vec{\Omega}' +$$

$$+ \int_{E'}\int_{\vec{\Omega}'}\Phi(E',\vec{\Omega}')\nu\Sigma_f(E')\chi(E)dE'd\vec{\Omega}' \qquad \text{EQN V-1}$$

This equation differs from Eqn. II-1 mainly in the "splitting up" of the generalized scattering cross section into two components. The first one represents all neutrons born by scattering events excluding fission, and the second term expresses explicitly the contribution due to fission neutrons born. We have also assumed that the inhomogeneous source $S(E,\vec{\Omega}) = 0$. In this equation,

$\Sigma(E) \equiv$ "collision cross section" and experimentally defined by

$$\text{transmission} = e^{-\Sigma(E)x}.$$

One often splits $\Sigma(E)$ into partial reaction cross sections $\Sigma_p(E)$ defined by the probability that a collision result in p is $\Sigma_p/\Sigma$. For example

$$\Sigma(E) = \Sigma^{n,n}(E) + \Sigma^{n,n'}(E) + \Sigma^{n,\gamma}(E) + \Sigma^{n,p}(E) + \Sigma^{n,2n}(E) + \Sigma^{n,f}(E) + \cdots$$

$\Sigma(E' \to E, \vec{\Omega}' \cdot \vec{\Omega}) \equiv$ "generalized scattering cross section exclusive of fission neutron production."

This same notation is often used to include fission neutrons (as indeed it was used in Eqn. II-1), but not here. One often splits $\Sigma(E' \to E, \vec{\Omega}' \cdot \vec{\Omega})$ into partial scattering cross sections representing the different reaction processes. Thus, if process p results in $N_p$ secondary neutrons with probability distribution in energy and angle given by $T_p(E', E, \vec{\Omega}' \cdot \vec{\Omega})$, then

$$\Sigma(E' \to E, \vec{\Omega}' \cdot \Omega) = \sum_p \Sigma_p(E') \cdot N_p \cdot T_p(E', E, \vec{\Omega}' \cdot \vec{\Omega}) =$$

$$= \Sigma^{n,2n}(E') \cdot 2 \cdot T_{n,2n}(E', E, \vec{\Omega}' \cdot \vec{\Omega}) + \Sigma^{n,n'}(E') \cdot 1 \cdot T_{n,n'}(E', E, \vec{\Omega}' \cdot \vec{\Omega}) +$$

$$+ \Sigma^{n,n}(E') \cdot 1 \cdot T_{n,n}(E', E, \vec{\Omega}' \cdot \vec{\Omega}) + \cdots\cdots$$

Sn-Input for 1-Table Consistent $P_o$ Approximation

$$\Sigma_g = \Sigma_g(o)$$

$$\Sigma^{(1)}_{g'\to g} = \Sigma_{o,g'\to g}(o) \qquad (g' \neq g)$$

$$\Sigma^{(1)}_{g\to g} = \Sigma_{o,g\to g}(o)$$

$$\Sigma_a = \Sigma_g - \left[\sum_{g'\neq g} \Sigma^{(1)}_{g\to g'} + \Sigma^{(1)}_{g\to g}\right]$$

Sn-Input for 2-Table Consistent $P_1$ Approximation

$$\Sigma_g = \Sigma_g(o)$$

$$\Sigma^{(1)}_{g'\to g} = \Sigma_{o,g'\to g}(o) \qquad (g' \neq g)$$

$$\Sigma^{(1)}_{g\to g} = \Sigma_{o,g\to g}(o)$$

$$\Sigma_a = \Sigma_g - \left[\sum_{g'\neq g} \Sigma^{(1)}_{g\to g'} + \Sigma^{(1)}_{g\to g}\right]$$

$$\Sigma^{(2)}_{g'\to g} = \Sigma_{1,g'\to g}(1) \qquad (g' \neq g)$$

$$\Sigma^{(2)}_{g\to g} = \Sigma_{1,g\to g}(1) + \left[\Sigma_g(o) - \Sigma_g(1)\right]$$

Sn-Input for 3-Table Consistent $P_2$ Approximation

$$\Sigma_g = \Sigma_g(o)$$

$$\Sigma^{(1)}_{g'\to g} = \Sigma_{o,g'\to g}(o) \qquad (g' \neq g)$$

$$\Sigma^{(1)}_{g\to g} = \Sigma_{o,g\to g}(o)$$

$$\Sigma_a = \Sigma_g - \left[\sum_{g'\neq g} \Sigma^{(1)}_{g\to g'} + \Sigma^{(1)}_{g\to g}\right]$$

$$\Sigma^{(2)}_{g'\to g} = \Sigma_{1,g'\to g}(1) \qquad (g' \neq g)$$

$$\Sigma^{(2)}_{g\to g} = \Sigma_{1,g\to g}(1) + \left[\Sigma_g(o) - \Sigma_g(1)\right]$$

$$\Sigma^{(3)}_{g'\to g} = \Sigma_{2,g'\to g}(2) \qquad (g' \neq g)$$

$$\Sigma^{(3)}_{g\to g} = \Sigma_{2,g\to g}(2) + \left[\Sigma_g(o) - \Sigma_g(2)\right]$$

## Sn-Input for 4-Table Consistent $P_3$ Approximation

$$\Sigma_g = \Sigma_g(o)$$

$$\Sigma^{(1)}_{g'\to g} = \Sigma_{o,g'\to g}(o) \qquad (g' \neq g)$$

$$\Sigma^{(1)}_{g\to g} = \Sigma_{o,g\to g}(o)$$

$$\Sigma_a = \Sigma_g - \left[\sum_{g'\neq g} \Sigma^{(1)}_{g\to g'} + \Sigma^{(1)}_{g\to g}\right]$$

$$\Sigma^{(2)}_{g'\to g} = \Sigma_{1,g'\to g}(1) \qquad (g' \neq g)$$

$$\Sigma^{(2)}_{g\to g} = \Sigma_{1,g\to g}(1) + \left[\Sigma_g(o) - \Sigma_g(1)\right]$$

$$\Sigma^{(3)}_{g'\to g} = \Sigma_{2,g'\to g}(2) \qquad (g' \neq g)$$

$$\Sigma^{(3)}_{g\to g} = \Sigma_{2,g\to g}(2) + \left[\Sigma_g(o) - \Sigma_g(2)\right]$$

$$\Sigma^{(4)}_{g'\to g} = \Sigma_{3,g'\to g}(3) \qquad (g' \neq g)$$

$$\Sigma^{(4)}_{g\to g} = \Sigma_{3,g\to g}(3) + \left[\Sigma_g(o) - \Sigma_g(3)\right]$$

Sn-Input for 5-Table Consistent $P_4$ Approximation

$$\Sigma_g = \Sigma_g(o)$$

$$\Sigma^{(1)}_{g'\to g} = \Sigma_{o,g'\to g}(o) \qquad (g' \neq g)$$

$$\Sigma^{(1)}_{g\to g} = \Sigma_{o,g\to g}(o)$$

$$\Sigma_a = \Sigma_g - \left[\sum_{g'\neq g} \Sigma^{(1)}_{g\to g'} + \Sigma^{(1)}_{g\to g}\right]$$

$$\Sigma^{(2)}_{g'\to g} = \Sigma_{1,g'\to g}(1) \qquad (g' = g)$$

$$\Sigma^{(2)}_{g\to g} = \Sigma_{1,g\to g}(1) + \left[\Sigma_g(o) - \Sigma_g(1)\right]$$

$$\Sigma^{(3)}_{g'\to g} = \Sigma_{2,g'\to g}(2) \qquad (g' \neq g)$$

$$\Sigma^{(3)}_{g\to g} = \Sigma_{2,g\to g}(2) + \left[\Sigma_g(o) - \Sigma_g(2)\right]$$

$$\Sigma^{(4)}_{g'\to g} = \Sigma_{3,g'\to g}(3) \qquad (g' \neq g)$$

$$\Sigma^{(4)}_{g\to g} = \Sigma_{3,g\to g}(3) + \left[\Sigma_g(o) - \Sigma_g(3)\right]$$

$$\Sigma^{(5)}_{g'\to g} = \Sigma_{4,g'\to g}(4) \qquad (g' \neq g)$$

$$\Sigma^{(5)}_{g\to g} = \Sigma_{4,g\to g}(4) + \left[\Sigma_g(o) - \Sigma_g(4)\right]$$

Sn-Input for 1-Table Transport Approximation (Isosource Transport)

$$\Sigma_{tr} = \Sigma_g(1) - \Sigma_{1,g}(1)$$

$$\Sigma^{(1)}_{g'\to g} = \Sigma_{o,g'\to g}(o) \qquad (g' \neq g)$$

$$\Sigma^{(1)}_{g\to g} = \Sigma_{o,g\to g}(o) + \left[\Sigma_g(1) - \Sigma_{1,g}(1) - \Sigma_g(o)\right]$$

$$\Sigma_a = \Sigma_{tr} - \left[\sum_{g'\neq g} \Sigma^{(1)}_{g\to g'} + \Sigma^{(1)}_{g\to g}\right]$$

Sn-Input for 2-Table Transport Approximation

$$\Sigma_g = \Sigma_g(2) - \Sigma_{2,g}(2)$$

$$\Sigma^{(1)}_{g'\to g} = \Sigma_{o,g'\to g}(o) \qquad (g' \neq g)$$

$$\Sigma^{(1)}_{g\to g} = \Sigma_{o,g\to g}(o) + \left[\Sigma_g(2) - \Sigma_{2,g}(2) - \Sigma_g(o)\right]$$

$$\Sigma_a = \Sigma_g - \left[\sum_{g'\neq g} \Sigma^{(1)}_{g\to g'} + \Sigma^{(1)}_{g\to g}\right]$$

$$\Sigma^{(2)}_{g'\to g} = \Sigma_{1,g'\to g}(1)$$

$$\Sigma^{(2)}_{g\to g} = \Sigma_{1,g\to g}(1) + \left[\Sigma_g(2) - \Sigma_{2,g}(2) - \Sigma_g(1)\right]$$

Sn-Input for 3-Table Transport Approximation

$$\Sigma_g = \Sigma_g(3) - \Sigma_{3,g}(3)$$

$$\Sigma^{(1)}_{g'\to g} = \Sigma_{o,g'\to g}(o) \qquad (g' \neq g)$$

$$\Sigma^{(1)}_{g\to g} = \Sigma_{o,g\to g}(o) + \left[\Sigma_g(3) - \Sigma_{3,g}(3) - \Sigma_g(o)\right]$$

$$\Sigma_a = \Sigma_g - \left[\sum_{g'\neq g} \Sigma^{(1)}_{g\to g'} + \Sigma^{(1)}_{g\to g}\right]$$

$$\Sigma^{(2)}_{g'\to g} = \Sigma_{1,g'\to g}(1) \qquad (g' \neq g)$$

$$\Sigma^{(2)}_{g\to g} = \Sigma_{1,g\to g}(1) + \left[\Sigma_g(3) - \Sigma_{3,g}(3) - \Sigma_g(1)\right]$$

$$\Sigma^{(3)}_{g'\to g} = \Sigma_{2,g'\to g}(2) \qquad (g' \neq g)$$

$$\Sigma^{(3)}_{g\to g} = \Sigma_{2,g'\to g}(2) + \left[\Sigma_g(3) - \Sigma_{3,g}(3) - \Sigma_g(2)\right]$$

## Sn-Input for 4-Table Transport Approximation

$$\Sigma_g = \Sigma_g(4) - \Sigma_{4,g}(4)$$

$$\Sigma^{(1)}_{g'\to g} = \Sigma_{o,g'\to g}(o) \qquad (g' \neq g)$$

$$\Sigma^{(1)}_{g\to g} = \Sigma_{o,g\to g}(o) + \left[\Sigma_g(4) - \Sigma_{4,g}(4) - \Sigma_g(o)\right]$$

$$\Sigma_a = \Sigma_g - \left[\sum_{g'\neq g} \Sigma^{(1)}_{g\to g'} + \Sigma^{(1)}_{g\to g}\right]$$

$$\Sigma^{(2)}_{g'\to g} = \Sigma_{1,g'\to g}(1) \qquad (g' \neq g)$$

$$\Sigma^{(2)}_{g\to g} = \Sigma_{1,g\to g}(1) + \left[\Sigma_g(4) - \Sigma_{4,g}(4) - \Sigma_g(1)\right]$$

$$\Sigma^{(3)}_{g'\to g} = \Sigma_{2,g'\to g}(2) \qquad (g' \neq g)$$

$$\Sigma^{(3)}_{g\to g} = \Sigma_{2,g\to g}(2) + \left[\Sigma_g(4) - \Sigma_{4,g}(4) - \Sigma_g(2)\right]$$

$$\Sigma^{(4)}_{g'\to g} = \Sigma_{3,g'\to g}(3) \qquad (g' \neq g)$$

$$\Sigma^{(4)}_{g\to g} = \Sigma_{3,g\to g}(3) + \left[\Sigma_g(4) - \Sigma_{4,g}(4) - \Sigma_g(3)\right]$$

Sn-Input for 5-Table Transport Approximation

$$\Sigma_g = \Sigma_g(5) - \Sigma_{5,g}(5)$$

$$\Sigma^{(1)}_{g'\to g} = \Sigma_{o,g'\to g}(o) \qquad (g' \neq g)$$

$$\Sigma^{(1)}_{g\to g} = \Sigma_{o,g\to g}(o) + \left[\Sigma_g(5) - \Sigma_{5,g}(5) - \Sigma_g(o)\right]$$

$$\Sigma_a = \Sigma_g - \left[\sum_{g'\neq g} \Sigma^{(1)}_{g\to g'} + \Sigma^{(1)}_{g\to g}\right]$$

$$\Sigma^{(2)}_{g'\to g} = \Sigma_{1,g'\to g}(1) \qquad (g' \neq g)$$

$$\Sigma^{(2)}_{g\to g} = \Sigma_{1,g\to g}(1) + \left[\Sigma_g(5) - \Sigma_{5,g}(5) - \Sigma_g(1)\right]$$

$$\Sigma^{(3)}_{g'\to g} = \Sigma_{2,g'\to g}(2) \qquad (g' \neq g)$$

$$\Sigma^{(3)}_{g\to g} = \Sigma_{2,g\to g}(2) + \left[\Sigma_g(5) - \Sigma_{5,g}(5) - \Sigma_g(2)\right]$$

$$\Sigma^{(4)}_{g'\to g} = \Sigma_{3,g'\to g}(3) \qquad (g' \neq g)$$

$$\Sigma^{(4)}_{g\to g} = \Sigma_{3,g\to g}(3) + \left[\Sigma_g(5) - \Sigma_{5,g}(5) - \Sigma_g(3)\right]$$

$$\Sigma^{(5)}_{g'\to g} = \Sigma_{4,g'\to g}(4) \qquad (g' \neq g)$$

$$\Sigma^{(5)}_{g\to g} = \Sigma_{4,g\to g}(4) + \left[\Sigma_g(5) - \Sigma_{5,g}(5) - \Sigma_g(4)\right]$$

V-4

Sn-Input for 1-Table Weapons Transport Approximation

$$\Sigma_g = \Sigma_g(o) - \Sigma_{1,g}(o)$$

$$\Sigma^{(1)}_{g'\to g} = \Sigma_{o,g'\to g}(o) - \Sigma_{1,g'\to g}(o) \qquad (g' \neq g)$$

$$\Sigma^{(1)}_{g\to g} = \Sigma_{o,g\to g}(o) - \Sigma_{1,g\to g}(o)$$

$$\Sigma_a = \Sigma_g - \left[\sum_{g'\neq g} \Sigma^{(1)}_{g\to g'} + \Sigma^{(1)}_{g\to g}\right]$$

Sn-Input for 2-Table $P_1$ Approximation (Bell)

$$\Sigma_g = \Sigma_g(o)$$

$$\Sigma^{(1)}_{g'\to g} = \Sigma_{o,g'\to g}(o) \qquad (g' \neq g)$$

$$\Sigma^{(1)}_{g\to g} = \Sigma_{o,g\to g}(o)$$

$$\Sigma_a = \Sigma_g - \left[\sum_{g'\neq g} \Sigma^{(1)}_{g\to g'} + \Sigma^{(1)}_{g\to g}\right]$$

$$\Sigma^{(2)}_{g'\to g} = \Sigma_{1,g'\to g}(o) \qquad (g' \neq g)$$

$$\Sigma^{(2)}_{g\to g} = \Sigma_{1,g\to g}(o)$$

TABLE V-1

25 GROUP STRUCTURE

| Group | Energy E | $\Delta E = E_n - E_{n+1}$ | $u = \ell n \frac{E_o}{E_n}$ ($E_o$ = 14 MeV) | $E_n/E_{n+1}$ | $\Delta u = \ell n \frac{E_n}{E_{n+1}}$ | $\bar{v}\left[\frac{cm}{sec}\right]$ x $10^{-8}$ |
|---|---|---|---|---|---|---|
| 1 | 12-14 MeV | 2 MeV | .1536 | 1.1666 | .1536 | 50 |
| 2 | 8.3-12 MeV | 3.7 MeV | .5222 | 1.4458 | .3686 | 43 |
| 3 | 5.3-8.3 MeV | 3 MeV | .9707 | 1.5660 | .4485 | 36 |
| 4 | 3.4-5.3 MeV | 1.9 MeV | 1.4146 | 1.5588 | .4439 | 29 |
| 5 | 2.2-3.4 MeV | 1.2 MeV | 1.8499 | 1.5455 | .4353 | 23 |
| 6 | 1.4-2.2 MeV | .8 MeV | 2.2999 | 1.5714 | .4520 | 19.0 |
| 7 | 0.9-1.4 MeV | .5 MeV | 2.7416 | 1.5556 | .4417 | 15.0 |
| 8 | 0.58-0.9 MeV | .32 MeV | 3.1809 | 1.5517 | .4393 | 12.0 |
| 9 | 370-580 KeV | 210 KeV | 3.6304 | 1.5676 | .4495 | 9.5 |
| 10 | 240-370 KeV | 130 KeV | 4.0633 | 1.5417 | .4329 | 7.6 |
| 11 | 150-240 KeV | 90 KeV | 4.5333 | 1.6000 | .4700 | 7.2 |
| 12 | 100-150 KeV | 50 KeV | 4.8387 | 1.5 | .4054 | 4.9 |
| 13 | 31.6-100 KeV | 69 KeV | 6.1098 | 3.2258 | 1.1711 | 3.28 |
| 14 | 10-31.6 KeV | 21 KeV | 7.2412 | 3.1 | 1.1314 | 1.78 |
| 15 | 3.16-10 KeV | 6.84 KeV | 8.3932 | 3.1646 | 1.1520 | 1.02 |
| 16 | 1-3.16 KeV | 2.16 KeV | 9.5437 | 3.16 | 1.1505 | .57 |
| 17 | .316-1 KeV | .684 KeV | 10.696 | 3.1646 | 1.1520 | .32 |
| 18 | 100-316 eV | 216 eV | 11.846 | 3.16 | 1.1505 | .16 |
| 19 | 31.6-100 eV | 68.4 eV | 12.998 | 3.1646 | 1.1520 | .10 |
| 20 | 10-31.6 eV | 21.6 eV | 14.149 | 3.16 | 1.1505 | .057 |
| 21 | 3.16-10 eV | 6.84 eV | 15.301 | 3.1646 | 1.1520 | .032 |
| 22 | 1-3.16 eV | 2.16 eV | 16.451 | 3.16 | 1.1505 | .018 |
| 23 | .316-1 eV | .684 eV | 17.603 | 3.1646 | 1.1520 | .010 |
| 24 | .026-.316 | .290 eV | 20.101 | 12.1538 | 2.4976 | .004 |
| 25 | Thermal .025-.026 eV | .001 eV | 20.14 | 1.04 | .0392 | .002 |

TABLE V-2

MACROSCOPIC CROSS SECTIONS OF AIR FOR 1-TABLE TRANSPORT COMPUTATIONS*

| g | $\Sigma_a$ | $\Sigma_g$ | $\Sigma^{(1)}_{g\to g}$ | $\Sigma^{(1)}_{g\to g+1}$ |
|---|---|---|---|---|
| 1 | 4.06 -6 | 5.000 -5 | 3.775 -6 | 1.349 -5 |
| 2 | 5.15 -6 | 4.701 -5 | 1.482 -5 | 9.515 -5 |
| 3 | 7.69 -6 | 5.576 -5 | 2.216 -5 | 2.291 -5 |
| 4 | 1.47 -5 | 7.590 -5 | 3.219 -5 | 2.877 -5 |
| 5 | 8.34 -6 | 6.523 -5 | 3.586 -5 | 2.102 -5 |
| 6 | 3.65 -6 | 8.491 -5 | 5.378 -5 | 2.748 -5 |
| 7 | 1.67 -6 | 9.458 -5 | 6.587 -5 | 2.704 -5 |
| 8 | 1.84 -6 | 9.471 -5 | 6.652 -5 | 2.636 -5 |
| 9 | 7.85 -7 | 1.315 -4 | 8.010 -5 | 5.065 -5 |
| 10 | 7.12 -8 | 1.572 -4 | 1.116 -4 | 4.557 -5 |
| 11 | 6.04 -8 | 1.692 -4 | 2.243 -4 | 4.480 -5 |
| 12 | 6.04 -8 | 1.860 -4 | 1.265 -4 | 5.947 -5 |
| 13 | 6.48 -8 | 2.242 -4 | 1.946 -4 | 2.958 -5 |
| 14 | 8.94 -8 | 2.550 -4 | 2.216 -4 | 3.328 -5 |
| 15 | 1.62 -7 | 2.822 -4 | 2.452 -4 | 3.681 -5 |
| 16 | 2.89 -7 | 3.232 -4 | 2.801 -4 | 4.286 -5 |
| 17 | 5.12 -7 | 3.686 -4 | 3.201 -4 | 4.790 -5 |
| 18 | 8.95 -7 | 4.003 -4 | 3.486 -4 | 5.079 -5 |
| 19 | 1.62 -6 | 4.162 -4 | 3.625 -4 | 5.214 -5 |
| 20 | 2.89 -6 | 4.242 -4 | 3.687 -4 | 5.261 -5 |
| 21 | 5.12 -6 | 4.317 -4 | 3.731 -4 | 5.352 -5 |
| 22 | 9.11 -6 | 4.396 -4 | 3.769 -4 | 5.357 -5 |
| 23 | 1.62 -5 | 4.451 -4 | 3.756 -4 | 5.332 -5 |
| 24 | 4.46 -5 | 4.838 -4 | 4.121 -4 | 2.712 -5 |
| 25 | 7.43 -5 | 5.362 -4 | 4.619 -4 | 0 |

*See Table V-6 for additional $\Sigma^{(1)}_{g\to g+2}$, $\Sigma^{(1)}_{g\to g+3}$, ..., associated with the isotropic inelastic and n,2n processes which are common to the first table of all multitable sets.

TABLE V-3

MACROSCOPIC CROSS SECTIONS OF AIR FOR 3-TABLE TRANSPORT COMPUTATIONS*

| g | $\Sigma_a$ | $\Sigma_g$ | $\Sigma^{(1)}_{g\to g}$ | $\Sigma^{(1)}_{g\to g+1}$ | $\Sigma^{(2)}_{g\to g}$ | $\Sigma^{(2)}_{g\to g+1}$ | $\Sigma^{(3)}_{g\to g}$ | $\Sigma^{(3)}_{g\to g+1}$ |
|---|---|---|---|---|---|---|---|---|
| 1 | 4.06 -6 | 6.171 -5 | 1.549 -5 | 1.349 -5 | 1.122 -5 | 4.912 -7 | 5.260 -6 | -6.806 -7 |
| 2 | 5.15 -6 | 5.548 -5 | 2.329 -5 | 9.515 -6 | 1.058 -5 | -2.108 -6 | 3.405 -6 | -1.594 -7 |
| 3 | 7.69 -6 | 5.798 -5 | 2.438 -5 | 2.291 -5 | 7.752 -6 | -5.532 -6 | 1.382 -6 | -1.683 -7 |
| 4 | 1.47 -5 | 6.761 -5 | 2.389 -5 | 2.877 -5 | -1.045 -6 | -7.248 -6 | -3.275 -6 | 1.348 -7 |
| 5 | 8.34 -6 | 6.209 -5 | 3.272 -5 | 2.102 -5 | 2.856 -6 | -5.998 -6 | -7.779 -7 | -1.354 -7 |
| 6 | 3.65 -6 | 8.832 -5 | 5.719 -5 | 2.748 -5 | 1.015 -5 | -6.742 -6 | 1.964 -6 | 1.146 -7 |
| 7 | 1.67 -6 | 9.320 -5 | 6.449 -5 | 2.704 -5 | 7.342 -6 | -8.727 -6 | 2.098 -6 | 9.585 -7 |
| 8 | 1.84 -6 | 1.011 -4 | 7.294 -5 | 2.636 -5 | 1.347 -5 | -7.049 -6 | 2.353 -6 | -5.923 -7 |
| 9 | 7.85 -7 | 1.274 -4 | 7.592 -5 | 5.065 -5 | 9.406 -6 | -1.359 -5 | -4.201 -6 | 6.366 -8 |
| 10 | 7.12 -8 | 1.560 -4 | 1.104 -4 | 4.557 -5 | 1.384 -5 | -1.507 -5 | -9.386 -7 | 3.476 -7 |
| 11 | 6.04 -8 | 1.741 -4 | 1.292 -4 | 4.480 -5 | 1.864 -5 | -1.374 -5 | -1.076 -7 | -1.815 -7 |
| 12 | 6.04 -8 | 1.947 -4 | 1.352 -4 | 5.947 -5 | 2.703 -5 | -1.834 -5 | 3.295 -7 | -3.639 -7 |
| 13 | 6.48 -8 | 2.326 -4 | 2.030 -4 | 2.958 -5 | 1.630 -5 | -7.906 -6 | -7.145 -7 | -4.162 -7 |
| 14 | 8.94 -8 | 2.673 -4 | 2.340 -4 | 3.328 -5 | 2.189 -5 | -9.546 -6 | 6.460 -7 | -5.338 -7 |
| 15 | 1.62 -7 | 2.954 -4 | 2.584 -4 | 3.681 -5 | 2.366 -5 | -1.044 -5 | 4.693 -7 | -5.595 -7 |
| 16 | 2.89 -7 | 3.378 -4 | 2.947 -4 | 4.282 -5 | 2.658 -5 | -1.194 -5 | 2.637 -7 | -6.228 -7 |
| 17 | 5.12 -7 | 3.860 -4 | 3.376 -4 | 4.790 -5 | 3.106 -5 | -1.360 -5 | 7.171 -7 | -7.521 -7 |
| 18 | 8.95 -7 | 4.200 -4 | 3.683 -4 | 5.079 -5 | 3.444 -5 | -1.474 -5 | 1.172 -6 | -8.451 -7 |
| 19 | 1.62 -6 | 4.368 -4 | 3.831 -4 | 5.214 -5 | 3.591 -5 | -1.531 -5 | 1.320 -6 | -9.085 -7 |
| 20 | 2.89 -6 | 4.452 -4 | 3.897 -4 | 5.261 -5 | 3.657 -5 | -1.558 -5 | 1.370 -6 | -9.243 -7 |
| 21 | 5.12 -6 | 4.529 -4 | 3.943 -4 | 5.352 -5 | 3.695 -5 | -1.574 -5 | 1.360 -6 | -9.325 -7 |
| 22 | 9.11 -6 | 4.611 -4 | 3.984 -4 | 5.357 -5 | 3.733 -5 | -1.587 -5 | 1.388 -6 | -9.315 -7 |
| 23 | 1.62 -5 | 4.665 -4 | 3.970 -4 | 5.332 -5 | 3.709 -5 | -1.573 -5 | 1.374 -6 | -9.281 -7 |
| 24 | 4.46 -5 | 5.032 -4 | 4.315 -4 | 2.712 -5 | 2.643 -5 | -6.994 -6 | -4.364 -7 | -3.318 -7 |
| 25 | 7.43 -5 | 5.592 -4 | 4.850 -4 | 0 | 2.300 -5 | 0 | 4.912 -7 | 0 |

*See Table V-6 for additional $\Sigma^{(1)}_{g\to g+2}$, $\Sigma^{(1)}_{g\to g+3}$, ..., associated with the isotropic inelastic and n,2n processes which are common to the first table of all multitable sets.

TABLE V-4

MACROSCOPIC CROSS SECTIONS OF AIR FOR 5-TABLE CONSISTENT COMPUTATIONS*

| g | $\Sigma_a$ | $\Sigma_g$ | $\Sigma^{(1)}_{g\to g}$ | $\Sigma^{(1)}_{g\to g+1}$ | $\Sigma^{(2)}_{g\to g}$ | $\Sigma^{(2)}_{g\to g+1}$ | $\Sigma^{(3)}_{g\to g}$ | $\Sigma^{(3)}_{g\to g+1}$ | $\Sigma^{(4)}_{g\to g}$ | $\Sigma^{(4)}_{g\to g+1}$ | $\Sigma^{(5)}_{g\to g}$ | $\Sigma^{(5)}_{g\to g+1}$ |
|---|---|---|---|---|---|---|---|---|---|---|---|---|
| 1 | 4.06 -6 | 7.819 -5 | 3.196 -5 | 1.349 -5 | 2.769 -5 | 4.912 -7 | 2.173 -5 | -6.806 -7 | 1.661 -5 | -1.400 -7 | 1.281 -5 | 7.502 -7 |
| 2 | 5.15 -6 | 7.063 -5 | 3.845 -5 | 9.515 -6 | 2.574 -5 | -2.108 -6 | 1.857 -5 | -1.593 -7 | 1.490 -5 | 2.624 -7 | 1.180 -5 | 3.571 -7 |
| 3 | 7.69 -6 | 6.964 -5 | 3.604 -5 | 2.291 -5 | 1.941 -5 | -5.532 -6 | 1.304 -5 | -1.683 -7 | 1.084 -5 | 8.193 -7 | 8.005 -6 | 1.206 -7 |
| 4 | 1.47 -5 | 9.338 -5 | 4.967 -5 | 2.877 -5 | 2.473 -5 | -7.248 -6 | 2.250 -5 | 1.348 -7 | 2.546 -5 | 3.136 -7 | 2.593 -5 | -1.526 -8 |
| 5 | 8.34 -6 | 7.611 -5 | 4.675 -5 | 2.102 -5 | 1.688 -5 | -5.998 -6 | 1.325 -5 | -1.354 -7 | 1.401 -5 | 1.687 -8 | 1.423 -5 | 9.537 -9 |
| 6 | 3.65 -6 | 9.797 -5 | 6.684 -5 | 2.748 -5 | 1.980 -5 | -6.742 -6 | 1.161 -5 | 1.146 -7 | 9.950 -6 | -3.032 -7 | 1.030 -5 | 5.232 -8 |
| 7 | 1.67 -6 | 1.198 -4 | 9.108 -5 | 2.704 -5 | 3.394 -5 | -8.727 -6 | 2.870 -5 | 9.585 -7 | 2.814 -5 | -1.547 -6 | 3.097 -5 | 1.740 -7 |
| 8 | 1.84 -6 | 1.083 -4 | 8.005 -5 | 2.636 -5 | 2.059 -5 | -7.049 -6 | 9.466 -6 | -5.923 -7 | 7.901 -6 | -7.880 -7 | 8.978 -6 | -1.063 -7 |
| 9 | 7.85 -7 | 1.719 -4 | 1.205 -4 | 5.065 -5 | 5.395 -5 | -1.359 -5 | 4.034 -5 | 6.366 -8 | 4.487 -5 | -3.326 -7 | 4.955 -5 | 7.205 -8 |
| 10 | 7.12 -8 | 1.570 -4 | 1.113 -4 | 4.557 -5 | 1.483 -5 | -1.507 -5 | 4.631 -8 | 3.476 -7 | 9.730 -7 | 1.188 -8 | 1.273 -6 | 1.647 -9 |
| 11 | 6.04 -8 | 1.749 -5 | 1.300 -4 | 4.480 -5 | 1.943 -5 | -1.374 -5 | 6.815 -7 | -1.815 -7 | 8.111 -7 | -2.201 -8 | 1.052 -6 | 2.872 -9 |
| 12 | 6.04 -8 | 1.954 -4 | 1.358 -4 | 5.947 -5 | 2.772 -5 | -1.834 -5 | 1.018 -6 | -3.639 -7 | 6.799 -7 | 8.878 -9 | 9.121 -7 | 1.671 -9 |
| 13 | 6.48 -8 | 2.366 -4 | 2.070 -4 | 2.958 -5 | 2.031 -5 | -7.906 -6 | 3.303 -6 | -4.162 -7 | 4.010 -6 | 7.129 -9 | 5.363 -6 | 2.562 -8 |
| 14 | 8.94 -8 | 2.678 -4 | 2.344 -4 | 3.328 -5 | 2.232 -5 | -9.546 -6 | 1.078 -6 | -5.338 -7 | 4.175 -7 | 1.440 -8 | 5.852 -7 | 1.931 -9 |
| 15 | 1.62 -7 | 2.966 -4 | 2.596 -4 | 3.681 -5 | 2.481 -5 | -1.044 -5 | 1.621 -6 | -5.595 -7 | 1.144 -6 | 7.760 -9 | 1.529 -6 | 8.241 -9 |
| 16 | 2.89 -7 | 3.399 -4 | 2.968 -4 | 4.282 -5 | 2.867 -5 | -1.194 -5 | 2.360 -6 | -6.228 -7 | 2.088 -6 | 8.463 -9 | 2.780 -6 | 1.005 -8 |
| 17 | 5.12 -7 | 3.873 -4 | 3.389 -4 | 4.790 -5 | 3.232 -5 | -1.360 -5 | 1.981 -6 | -7.521 -7 | 1.262 -6 | 1.825 -9 | 1.677 -6 | 1.085 -8 |
| 18 | 8.95 -7 | 4.203 -4 | 3.686 -4 | 5.080 -5 | 3.471 -5 | -1.474 -5 | 1.442 -6 | -8.451 -7 | 2.663 -7 | 3.437 -9 | 3.497 -7 | 1.831 -8 |
| 19 | 1.62 -6 | 4.369 -4 | 3.831 -4 | 5.214 -5 | 3.597 -5 | -1.531 -5 | 1.386 -6 | -9.085 -7 | 5.587 -8 | 9.707 -9 | 7.558 -8 | 1.999 -8 |
| 20 | 2.89 -6 | 4.452 -4 | 3.897 -4 | 5.261 -5 | 3.655 -5 | -1.558 -5 | 1.352 -6 | -9.243 -7 | -3.021 -8 | 1.220 -8 | -4.762 -8 | 3.282 -8 |
| 21 | 5.12 -6 | 4.530 -4 | 3.943 -4 | 5.352 -5 | 3.701 -5 | -1.574 -5 | 1.421 -6 | -9.325 -7 | 5.404 -8 | 6.965 -9 | 7.055 -8 | 1.835 -8 |
| 22 | 9.11 -6 | 4.610 -4 | 3.984 -4 | 5.357 -5 | 3.731 -5 | -1.587 -5 | 1.370 -6 | -9.315 -7 | -3.481 -8 | 1.666 -8 | -3.799 -8 | 2.259 -8 |
| 23 | 1.62 -5 | 4.665 -4 | 3.970 -4 | 5.332 -5 | 3.710 -5 | -1.573 -5 | 1.382 -6 | -9.281 -7 | -5.403 -9 | 1.379 -8 | 1.396 -8 | 6.186 -9 |
| 24 | 4.46 -5 | 5.070 -4 | 4.353 -4 | 2.712 -5 | 3.021 -5 | -6.994 -6 | 3.349 -6 | -3.318 -7 | 3.762 -6 | 2.353 -8 | 4.964 -6 | 2.850 -8 |
| 25 | 7.43 -5 | 5.592 -4 | 4.849 -4 | 0 | 2.298 -5 | 0 | 4.662 -7 | 0 | 2.497 -8 | 0 | -2.554 -8 | 0 |

*See Table V-6 for additional $\Sigma^{(1)}_{g\to g+2}$, $\Sigma^{(1)}_{g\to g+3}$, ···, associated with the isotropic inelastic and n,2n processes which are common to the first table of all multitable sets.

TABLE V-5

MACROSCOPIC CROSS SECTIONS OF AIR FOR 5-TABLE TRANSPORT COMPUTATIONS*

| g | $\Sigma_a$ | $\Sigma_g$ | $\Sigma^{(1)}_{g\to g}$ | $\Sigma^{(1)}_{g\to g+1}$ | $\Sigma^{(2)}_{g\to g}$ | $\Sigma^{(2)}_{g\to g+1}$ | $\Sigma^{(3)}_{g\to g}$ | $\Sigma^{(3)}_{g\to g+1}$ | $\Sigma^{(4)}_{g\to g}$ | $\Sigma^{(4)}_{g\to g+1}$ | $\Sigma^{(5)}_{g\to g}$ | $\Sigma^{(5)}_{g\to g+1}$ |
|---|---|---|---|---|---|---|---|---|---|---|---|---|
| 1 | 4.06 -6 | 6.830 -5 | 2.207 -5 | 1.349 -5 | 1.781 -5 | 4.912 -7 | 1.185 -5 | -6.806 -7 | 6.726 -6 | -1.400 -7 | 2.926 -6 | 7.502 -7 |
| 2 | 5.15 -6 | 6.234 -5 | 3.015 -5 | 9.515 -6 | 1.744 -5 | -2.108 -6 | 1.027 -5 | -1.594 -7 | 6.606 -6 | 2.624 -7 | 3.504 -6 | 3.571 -7 |
| 3 | 7.69 -6 | 6.502 -5 | 3.142 -5 | 2.291 -5 | 1.479 -5 | -3.532 -6 | 8.422 -6 | -1.683 -7 | 6.221 -6 | 8.193 -7 | 3.384 -6 | 1.206 -7 |
| 4 | 1.47 -5 | 6.609 -5 | 2.238 -5 | 2.877 -5 | -2.554 -6 | -7.248 -6 | -4.784 -6 | 1.348 -7 | -1.823 -6 | 3.136 -7 | -1.351 -6 | -1.526 -8 |
| 5 | 8.34 -6 | 6.163 -5 | 3.227 -5 | 2.102 -5 | 2.403 -6 | -5.998 -6 | -1.231 -6 | -1.354 -7 | -4.697 -7 | 1.687 -8 | -2.517 -7 | 9.537 -9 |
| 6 | 3.65 -6 | 8.656 -5 | 5.543 -5 | 2.748 -5 | 8.389 -6 | -6.742 -6 | 2.064 -7 | 1.146 -7 | -1.455 -6 | -3.032 -7 | -1.107 -6 | 5.232 -8 |
| 7 | 1.67 -6 | 8.451 -5 | 5.580 -5 | 2.704 -5 | -1.342 -6 | -8.727 -6 | -6.586 -6 | 9.585 -7 | -7.138 -6 | -1.547 -6 | -4.310 -6 | 1.740 -7 |
| 8 | 1.84 -6 | 9.751 -5 | 6.932 -5 | 2.636 -5 | 9.847 -6 | -7.049 -6 | -1.272 -6 | -5.923 -7 | -2.837 -6 | -7.880 -7 | -1.760 -6 | -1.063 -7 |
| 9 | 7.85 -7 | 1.183 -4 | 6.682 -5 | 5.065 -5 | 3.097 -7 | -1.359 -5 | -1.330 -5 | 6.366 -8 | -8.764 -6 | -3.326 -7 | -4.086 -6 | 7.205 -8 |
| 10 | 7.12 -8 | 1.554 -4 | 1.098 -4 | 4.557 -5 | 1.325 -5 | -1.507 -5 | -1.528 -5 | 3.476 -8 | -6.017 -7 | 1.188 -8 | -3.019 -7 | 1.647 -9 |
| 11 | 6.04 -8 | 1.735 -4 | 1.287 -4 | 4.480 -5 | 1.812 -5 | -1.374 -5 | -6.278 -7 | -1.815 -7 | -4.982 -7 | -2.201 -8 | -2.573 -7 | 2.872 -9 |
| 12 | 6.04 -8 | 1.942 -4 | 1.347 -4 | 5.947 -5 | 2.658 -5 | -1.834 -5 | -1.179 -7 | -3.639 -7 | -4.562 -7 | 8.878 -9 | -2.240 -7 | 1.671 -9 |
| 13 | 6.48 -8 | 2.299 -4 | 2.002 -4 | 2.958 -5 | 1.356 -5 | -7.906 -6 | -3.451 -6 | -4.162 -7 | -2.743 -6 | 7.129 -9 | -1.391 -6 | 2.562 -8 |
| 14 | 8.94 -8 | 2.670 -4 | 2.336 -4 | 3.328 -5 | 2.158 -5 | -9.546 -6 | 3.365 -7 | -5.338 -7 | -3.240 -7 | 1.440 -8 | -1.563 -7 | 1.931 -9 |
| 15 | 1.62 -7 | 2.946 -4 | 2.577 -4 | 3.681 -5 | 2.289 -5 | -1.044 -5 | -2.990 -7 | -5.595 -7 | -7.761 -7 | 7.760 -9 | -3.911 -7 | 8.241 -9 |
| 16 | 2.89 -7 | 3.364 -4 | 2.933 -4 | 4.282 -5 | 2.520 -5 | -1.194 -5 | -1.116 -6 | -6.228 -7 | -1.388 -6 | 8.463 -9 | -6.959 -7 | 1.005 -8 |
| 17 | 5.12 -7 | 3.852 -4 | 3.368 -4 | 4.790 -5 | 3.021 -5 | -1.360 -5 | -1.277 -7 | -7.521 -7 | -8.467 -7 | 1.825 -9 | -4.321 -7 | 1.085 -8 |
| 18 | 8.95 -7 | 4.198 -4 | 3.681 -4 | 5.079 -5 | 3.425 -5 | -1.474 -5 | 9.754 -7 | -8.451 -7 | -2.002 -7 | 3.437 -9 | -1.168 -7 | 1.831 -8 |
| 19 | 1.62 -6 | 4.367 -4 | 3.830 -4 | 5.214 -5 | 3.585 -5 | -1.531 -5 | 1.260 -6 | -9.085 -7 | -7.004 -8 | 9.707 -9 | -5.033 -8 | 1.999 -8 |
| 20 | 2.89 -6 | 4.452 -4 | 3.897 -4 | 5.261 -5 | 3.657 -5 | -1.558 -5 | 1.364 -6 | -9.243 -7 | -1.894 -8 | 1.220 -8 | -3.635 -8 | 3.282 -8 |
| 21 | 5.12 -6 | 4.528 -4 | 3.942 -4 | 5.352 -5 | 3.689 -5 | -1.574 -5 | 1.303 -6 | -9.325 -7 | -6.320 -8 | 6.965 -9 | -4.670 -8 | 1.835 -8 |
| 22 | 9.11 -6 | 4.610 -4 | 3.984 -4 | 5.357 -5 | 3.732 -5 | -1.587 -5 | 1.382 -6 | -9.315 -7 | -2.274 -8 | 1.666 -8 | -2.991 -8 | 2.259 -8 |
| 23 | 1.62 -5 | 4.665 -4 | 3.970 -4 | 5.332 -5 | 3.707 -5 | -1.573 -5 | 1.350 -6 | -9.281 -7 | -3.758 -8 | 1.379 -8 | -1.822 -8 | 6.186 -9 |
| 24 | 4.46 -5 | 5.009 -4 | 4.291 -4 | 2.712 -5 | 2.404 -5 | -6.994 -6 | -2.819 -6 | -3.318 -7 | -2.407 -6 | 2.353 -8 | -1.204 -6 | 2.850 -8 |
| 25 | 7.43 -5 | 5.592 -4 | 4.850 -4 | 0 | 2.300 -5 | 0 | 4.910 -7 | 0 | -1.876 -10 | 0 | -7.579 -10 | 0 |

*See Table V-6 for additional $\Sigma^{(1)}_{g\to g+2}$, $\Sigma^{(1)}_{g\to g+3}$, ···, associated with the isotropic inelastic and n,2n processes which are common to the first table of all multitable sets.

TABLE V-6

MACROSCOPIC TRANSFER CROSS SECTIONS OF AIR ASSOCIATED WITH THE ISOTROPIC INELASTIC AND n,2n PROCESSES WHICH ARE COMMON TO THE FIRST TABLE OF ALL MULTITABLE SETS

| g | $\Sigma^{(1)}_{g\to g+2}$ | $\Sigma^{(1)}_{g\to g+3}$ | $\Sigma^{(1)}_{g\to g+4}$ | $\Sigma^{(1)}_{g\to g+5}$ | $\Sigma^{(1)}_{g\to g+6}$ | $\Sigma^{(1)}_{g\to g+7}$ | $\Sigma^{(1)}_{g\to g+8}$ | $\Sigma^{(1)}_{g\to g+9}$ | $\Sigma^{(1)}_{g\to g+10}$ | $\Sigma^{(1)}_{g\to g+11}$ | $\Sigma^{(1)}_{g\to g+12}$ | $\Sigma^{(1)}_{g\to g+13}$ |
|---|---|---|---|---|---|---|---|---|---|---|---|---|
| 1 | 5.191 -6 | 7.588 -6 | 5.161 -6 | 5.140 -6 | 3.625 -6 | 1.067 -6 | 4.496 -7 | 2.052 -7 | 1.815 -7 | 4.658 -8 | 2.035 -8 | 2.131 -9 |
| 2 | 2.972 -6 | 4.736 -6 | 4.338 -6 | 3.223 -6 | 1.439 -6 | 6.193 -7 | 1.132 -7 | 5.009 -8 | 1.783 -8 | 1.289 -8 | 1.223 -9 | 1.266 -10 |
| 3 | 7.979 -7 | 6.210 -7 | 6.898 -7 | 7.045 -7 | 1.669 -7 | 6.749 -9 | 0 | 0 | 0 | 0 | 0 | 0 |
| 4 | 1.447 -7 | 7.818 -8 | 9.580 -9 | 0 | | | | | | | | |
| 5 | 0 | 1.171 -8 | 0 | | | | | | | | | |

## VI. FAST NEUTRON PENETRATION IN SEA LEVEL AIR

In order to illustrate the relative accuracies of the various multitable-multigroup cross section sets, we chose the test problem of a 1000 meter radius sphere of sea level air containing a unit group 1 neutron source distributed over a central sphere of 10 meter radius. Twenty five group flux distributions were then computed by Sn, in order n = 16, for all multitable cross section recipes listed in Chapter V. Tables VI-1 through VI-3 list the computed total fluxes at 110, 525, and 825 meters. The dependence of computed group fluxes on multitable recipes is most pronounced for the top group. Figure VI-1 graphs computed group 1 fluxes at 825 meters against table length. Here it may be seen that all computed fluxes, save those of 1-table consistent $P_o$, agree with the presumably most accurate 5-table transport values to within 10%; if one further excludes 2- and 3-table consistent $P_{K-1}$ computations, the agreements are within 5%. Specifically one sees that the historical 1-table transport approximation furnishes a relatively good computational basis for neutron penetration in air (of course one should not assume comparable accuracy of the 1-table transport approximation for all neutron penetration problems).

All computations of the above test problem were based on the same microscopic cross section data. The uncertainty in, say, the computed

value of group 1 flux at a large distance from the source due to uncertainty in the microscopic cross section data may be estimated from the asymptotic flux solution $\Phi_1 \sim e^{-K_1 R}/R$ which implies $\delta\Phi_1/\Phi_1 = (K_1 R)\delta K_1/K_1$. Qualitatively, the uncertainty $\delta K_1/K_1$ in the propagation number $K_1$ is equal to the uncertainty $\delta\sigma/\sigma$ in the group 1 microscopic cross sections. For sea level air, $K_1 \simeq 0.006$/meter, and thus a 1% uncertainty in group 1 cross sections reflects already at R = 1000 meters a 6% uncertainty in group 1 flux.

The bases for our final numerical evaluations of neutron penetration in air were chosen as 1) a 3000 meter radius sphere of sea level air with a unit group 1 neutron source distributed over a central sphere of 10 meter radius, 2) the 5 table transport-25 group cross section set, and 3) Sn computation in order n = 16 and with 170 space points. This "problem" essentially exhausts the capacity of the Los Alamos Stretch computer, and indeed this was our intention. Figures VI-2 and VI-3 give histogrammed flux spectra computed at 110, 525, 825, and 1825 meters. Figures VI-4 and VI-5 show the spatial dependence of the computed neutron fluxes out to 3000 meters.

TABLE VI-1

NEUTRON FLUX IN ENERGY GROUP g, SEA LEVEL AIR AT R = 110 METERS DUE TO VOLUME SOURCE R = 10 METERS,
1 NEUTRON GP 1 (12-14 MEV)

$\Phi_g$ (110 meter)

| g | 1-TABLE | | 2-TABLE | | 3-TABLE | | 4-TABLE | | 5-TABLE | |
|---|---|---|---|---|---|---|---|---|---|---|
| | CONST | TR | CONST | TR | CONST | TR | CONST | TR | CONST | TR |
| 1 | 4.77 -10 | 4.22 -10 | 4.19 -10 | 4.20 -10 | 4.07 -10 | 4.19 -10 | 4.14 -10 | 4.20 -10 | 4.22 -10 | 4.20 -10 |
| 2 | 1.36 -10 | 1.12 -10 | 9.99 -11 | 1.06 -10 | 1.04 -10 | 1.06 -10 | 1.04 -10 | 1.06 -10 | 1.07 -10 | 1.06 -10 |
| 3 | 7.20 -11 | 6.04 -11 | 5.59 -11 | 5.89 -11 | 5.80 -11 | 5.89 -11 | 5.81 -11 | 5.90 -11 | 5.93 -11 | 5.91 -11 |
| 4 | 9.95 -11 | 8.41 -11 | 7.83 -11 | 8.24 -11 | 8.11 -11 | 8.23 -11 | 8.12 -11 | 8.25 -11 | 8.29 -11 | 8.26 -11 |
| 5 | 1.20 -10 | 1.01 -10 | 9.46 -11 | 9.96 -11 | 9.84 -11 | 9.96 -11 | 9.82 -11 | 9.98 -11 | 1.00 -10 | 9.99 -11 |
| 6 | 1.18 -10 | 9.95 -11 | 9.40 -11 | 9.82 -11 | 9.67 -11 | 9.82 -11 | 9.71 -11 | 9.84 -11 | 9.90 -11 | 9.85 -11 |
| 7 | 1.24 -10 | 1.02 -10 | 9.50 -11 | 1.00 -10 | 9.86 -11 | 1.00 -10 | 9.88 -11 | 1.00 -10 | 1.01 -10 | 1.00 -10 |
| 8 | 8.90 -11 | 7.24 -11 | 6.96 -11 | 7.27 -11 | 7.18 -11 | 7.28 -11 | 7.20 -11 | 7.29 -11 | 7.35 -11 | 7.30 -11 |
| 9 | 4.21 -11 | 3.33 -11 | 3.22 -11 | 3.36 -11 | 3.32 -11 | 3.37 -11 | 3.33 -11 | 3.37 -11 | 3.40 -11 | 3.38 -11 |
| 10 | 3.85 -11 | 3.11 -11 | 3.02 -11 | 3.14 -11 | 3.10 -11 | 3.14 -11 | 3.11 -11 | 3.15 -11 | 3.17 -11 | 3.15 -11 |
| 11 | 3.33 -11 | 2.72 -11 | 2.67 -11 | 2.76 -11 | 2.72 -11 | 2.76 -11 | 2.73 -11 | 2.76 -11 | 2.79 -11 | 2.76 -11 |
| 12 | 2.21 -11 | 1.81 -11 | 1.78 -11 | 1.83 -11 | 1.81 -11 | 1.83 -11 | 1.82 -11 | 1.83 -11 | 1.85 -11 | 1.84 -11 |
| 13 | 3.62 -11 | 2.97 -11 | 2.93 -11 | 3.01 -11 | 2.98 -11 | 3.01 -11 | 2.99 -11 | 3.02 -11 | 3.05 -11 | 3.02 -11 |
| 14 | 2.76 -11 | 2.27 -11 | 2.24 -11 | 2.30 -11 | 2.27 -11 | 2.30 -11 | 2.29 -11 | 2.30 -11 | 2.32 -11 | 2.30 -11 |
| 15 | 2.22 -11 | 1.82 -11 | 1.81 -11 | 1.85 -11 | 1.83 -11 | 1.85 -11 | 1.83 -11 | 1.85 -11 | 1.87 -11 | 1.85 -11 |
| 16 | 1.75 -11 | 1.44 -11 | 1.43 -11 | 1.46 -11 | 1.44 -11 | 1.46 -11 | 1.45 -11 | 1.46 -11 | 1.47 -11 | 1.46 -11 |
| 17 | 1.46 -11 | 1.20 -11 | 1.19 -11 | 1.21 -11 | 1.20 -11 | 1.21 -11 | 1.21 -11 | 1.22 -11 | 1.23 -11 | 1.22 -11 |
| 18 | 1.26 -11 | 1.06 -11 | 1.05 -11 | 1.07 -11 | 1.06 -11 | 1.07 -11 | 1.07 -11 | 1.07 -11 | 1.09 -11 | 1.07 -11 |
| 19 | 1.16 -11 | 9.62 -12 | 9.55 -12 | 9.71 -12 | 9.62 -12 | 9.71 -12 | 9.65 -12 | 9.72 -12 | 9.83 -12 | 9.73 -12 |
| 20 | 1.05 -11 | 8.70 -12 | 8.64 -12 | 8.78 -12 | 8.70 -12 | 8.78 -12 | 8.72 -12 | 8.78 -12 | 8.88 -12 | 8.80 -12 |
| 21 | 9.10 -12 | 7.54 -12 | 7.49 -12 | 7.60 -12 | 7.54 -12 | 7.60 -12 | 7.56 -12 | 7.61 -12 | 7.70 -12 | 7.63 -12 |
| 22 | 7.53 -12 | 6.24 -12 | 6.21 -12 | 6.30 -12 | 6.25 -12 | 6.30 -12 | 6.26 -12 | 6.30 -12 | 6.38 -12 | 6.31 -12 |
| 23 | 5.65 -12 | 4.69 -12 | 4.66 -12 | 4.73 -12 | 4.69 -12 | 4.73 -12 | 4.70 -12 | 4.73 -12 | 4.79 -12 | 4.74 -12 |
| 24 | 4.10 -12 | 3.40 -12 | 3.39 -12 | 3.43 -12 | 3.40 -12 | 3.43 -12 | 3.41 -12 | 3.43 -12 | 3.48 -12 | 3.44 -12 |
| 25 | 1.47 -12 | 1.22 -12 | 1.21 -12 | 1.23 -12 | 1.22 -12 | 1.23 -12 | 1.22 -12 | 1.23 -12 | 1.25 -12 | 1.23 -12 |

TABLE VI-2

NEUTRON FLUX IN ENERGY GROUP g, SEA LEVEL AIR AT R = 525 METERS DUE TO VOLUME SOURCE R = 10 METERS, 1 NEUTRON GP 1 (12-14 MEV)

$\Phi_g$ (525 meter)

| | 1-TABLE | | 2-TABLE | | 3-TABLE | | 4-TABLE | | 5-TABLE | |
|---|---|---|---|---|---|---|---|---|---|---|
| g | CONST | TR | CONST | TR | CONST | TR | CONST | TR | CONST | TR |
| 1 | 1.60 -12 | 2.38 -12 | 2.54 -12 | 2.43 -12 | 2.58 -12 | 2.43 -12 | 2.50 -12 | 2.42 -12 | 2.47 -12 | 2.44 -12 |
| 2 | 1.95 -12 | 2.29 -12 | 2.48 -12 | 2.37 -12 | 2.39 -12 | 2.37 -12 | 2.39 -12 | 2.37 -12 | 2.42 -12 | 2.39 -12 |
| 3 | 1.52 -12 | 1.66 -12 | 1.75 -12 | 1.69 -12 | 1.70 -12 | 1.69 -12 | 1.69 -12 | 1.68 -12 | 1.71 -12 | 1.69 -12 |
| 4 | 1.79 -12 | 2.00 -12 | 2.10 -12 | 2.03 -12 | 2.05 -12 | 2.03 -12 | 2.04 -12 | 2.02 -12 | 2.07 -12 | 2.03 -12 |
| 5 | 3.83 -12 | 4.01 -12 | 4.12 -12 | 4.01 -12 | 4.03 -12 | 4.01 -12 | 4.02 -12 | 4.01 -12 | 4.08 -12 | 4.02 -12 |
| 6 | 4.25 -12 | 4.39 -12 | 4.49 -12 | 4.40 -12 | 4.41 -12 | 4.39 -12 | 4.41 -12 | 4.39 -12 | 4.47 -12 | 4.41 -12 |
| 7 | 5.63 -12 | 5.76 -12 | 5.88 -12 | 5.76 -12 | 5.78 -12 | 5.76 -12 | 5.77 -12 | 5.76 -12 | 5.86 -12 | 5.77 -12 |
| 8 | 6.52 -12 | 6.42 -12 | 6.47 -12 | 6.39 -12 | 6.38 -12 | 6.38 -12 | 6.38 -12 | 6.38 -12 | 6.48 -12 | 6.40 -12 |
| 9 | 3.54 -12 | 3.46 -12 | 3.48 -12 | 3.44 -12 | 3.44 -12 | 3.44 -12 | 3.44 -12 | 3.44 -12 | 3.49 -12 | 3.45 -12 |
| 10 | 4.11 -12 | 3.95 -12 | 3.96 -12 | 3.93 -12 | 3.92 -12 | 3.93 -12 | 3.92 -12 | 3.92 -12 | 3.99 -12 | 3.94 -12 |
| 11 | 4.30 -12 | 4.09 -12 | 4.09 -12 | 4.06 -12 | 4.05 -12 | 4.06 -12 | 4.06 -12 | 4.06 -12 | 4.12 -12 | 4.07 -12 |
| 12 | 3.29 -12 | 3.10 -12 | 3.10 -12 | 3.08 -12 | 3.07 -12 | 3.08 -12 | 3.07 -12 | 3.08 -12 | 3.13 -12 | 3.09 -12 |
| 13 | 6.67 -12 | 6.23 -12 | 6.22 -12 | 6.19 -12 | 6.17 -12 | 6.19 -12 | 6.18 -12 | 6.19 -12 | 6.28 -12 | 6.20 -12 |
| 14 | 5.93 -12 | 5.49 -12 | 5.48 -12 | 5.47 -12 | 5.44 -12 | 5.46 -12 | 5.45 -12 | 5.46 -12 | 5.54 -12 | 5.48 -12 |
| 15 | 5.33 -12 | 4.91 -12 | 4.89 -12 | 4.89 -12 | 4.87 -12 | 4.88 -12 | 4.87 -12 | 4.88 -12 | 4.96 -12 | 4.90 -12 |
| 16 | 4.53 -12 | 4.16 -12 | 4.15 -12 | 4.14 -12 | 4.13 -12 | 4.14 -12 | 4.13 -12 | 4.14 -12 | 4.20 -12 | 4.15 -12 |
| 17 | 3.99 -12 | 3.66 -12 | 3.64 -12 | 3.64 -12 | 3.63 -12 | 3.64 -12 | 3.63 -12 | 3.64 -12 | 3.69 -12 | 3.65 -12 |
| 18 | 3.68 -12 | 3.36 -12 | 3.35 -12 | 3.35 -12 | 3.34 -12 | 3.35 -12 | 3.34 -12 | 3.35 -12 | 3.40 -12 | 3.36 -12 |
| 19 | 3.46 -12 | 3.16 -12 | 3.15 -12 | 3.15 -12 | 3.13 -12 | 3.15 -12 | 3.14 -12 | 3.15 -12 | 3.19 -12 | 3.15 -12 |
| 20 | 3.24 -12 | 2.95 -12 | 2.94 -12 | 2.94 -12 | 2.92 -12 | 2.94 -12 | 2.93 -12 | 2.94 -12 | 2.98 -12 | 2.94 -12 |
| 21 | 2.89 -12 | 2.62 -12 | 2.62 -12 | 2.62 -12 | 2.61 -12 | 2.62 -12 | 2.61 -12 | 2.62 -12 | 2.66 -12 | 2.62 -12 |
| 22 | 7.89 -12 | 2.23 -12 | 2.22 -12 | 2.22 -12 | 2.21 -12 | 2.22 -12 | 2.22 -12 | 2.22 -12 | 2.25 -12 | 2.23 -12 |
| 23 | 5.91 -12 | 1.71 -12 | 1.70 -12 | 1.70 -12 | 1.69 -12 | 1.70 -12 | 1.70 -12 | 1.70 -12 | 1.73 -12 | 1.70 -12 |
| 24 | 4.28 -12 | 1.26 -12 | 1.26 -12 | 1.26 -12 | 1.25 -12 | 1.26 -12 | 1.25 -12 | 1.26 -12 | 1.28 -12 | 1.26 -12 |
| 25 | 1.53 -12 | 4.58 -13 | 4.57 -13 | 4.57 -13 | 4.55 -13 | 4.57 -13 | 4.56 -13 | 4.57 -13 | 4.64 -13 | 4.58 -13 |

TABLE VI-3

NEUTRON FLUX IN ENERGY GROUP g, SEA LEVEL AIR AT R = 825 METERS DUE TO VOLUME SOURCE R = 10 METERS,
1 NEUTRON GP 1 (12-14 MEV)

$\phi_g$ (825 meter)

| | 1-TABLE | | 2-TABLE | | 3-TABLE | | 4-TABLE | | 5-TABLE | |
|---|---|---|---|---|---|---|---|---|---|---|
| g | CONST | TR | CONST | TR | CONST | TR | CONST | TR | CONST | TR |
| 1 | 7.69 -14 | 2.09 -13 | 1.93 -13 | 2.06 -13 | 2.23 -13 | 2.08 -13 | 2.18 -13 | 2.08 -13 | 2.13 -13 | 2.10 -13 |
| 2 | 1.62 -13 | 2.95 -13 | 3.24 -13 | 3.15 -13 | 3.24 -13 | 3.15 -13 | 3.20 -13 | 3.15 -13 | 3.23 -13 | 3.18 -13 |
| 3 | 1.51 -13 | 2.28 -13 | 2.43 -13 | 2.37 -13 | 2.42 -13 | 2.37 -13 | 2.40 -13 | 2.37 -13 | 2.42 -13 | 2.39 -13 |
| 4 | 1.63 -13 | 2.51 -13 | 2.63 -13 | 2.58 -13 | 2.65 -13 | 2.59 -13 | 2.63 -13 | 2.58 -13 | 2.65 -13 | 2.60 -13 |
| 5 | 4.31 -13 | 5.80 -13 | 6.12 -13 | 5.97 -13 | 6.08 -13 | 5.98 -13 | 6.03 -13 | 5.97 -13 | 6.11 -13 | 6.00 -13 |
| 6 | 5.03 -13 | 6.54 -13 | 6.77 -13 | 6.63 -13 | 6.74 -13 | 6.64 -13 | 6.70 -13 | 6.63 -13 | 6.78 -13 | 6.67 -13 |
| 7 | 7.06 -13 | 9.08 -13 | 9.43 -13 | 9.24 -13 | 9.36 -13 | 9.24 -13 | 9.31 -13 | 9.24 -13 | 9.44 -13 | 9.27 -13 |
| 8 | 9.31 -13 | 1.12 -12 | 1.15 -12 | 1.13 -12 | 1.14 -12 | 1.13 -12 | 1.13 -12 | 1.13 -12 | 1.15 -12 | 1.13 -12 |
| 9 | 5.22 -13 | 6.25 -13 | 6.37 -13 | 6.25 -13 | 6.30 -13 | 6.25 -13 | 6.28 -13 | 6.25 -13 | 6.38 -13 | 6.27 -13 |
| 10 | 6.38 -13 | 7.38 -13 | 7.51 -13 | 7.37 -13 | 7.42 -13 | 7.37 -13 | 7.40 -13 | 7.37 -13 | 7.52 -13 | 7.40 -13 |
| 11 | 7.01 -13 | 7.90 -13 | 8.01 -13 | 7.87 -13 | 7.92 -13 | 7.87 -13 | 7.90 -13 | 7.87 -13 | 8.02 -13 | 7.89 -13 |
| 12 | 5.54 -13 | 6.13 -13 | 6.21 -13 | 6.11 -13 | 6.14 -13 | 6.11 -13 | 6.13 -13 | 6.11 -13 | 6.22 -13 | 6.13 -13 |
| 13 | 1.19 -12 | 1.29 -12 | 1.30 -12 | 1.28 -12 | 1.28 -12 | 1.28 -12 | 1.28 -12 | 1.28 -12 | 1.30 -12 | 1.28 -12 |
| 14 | 1.11 -12 | 1.17 -12 | 1.18 -12 | 1.17 -12 | 1.17 -12 | 1.17 -12 | 1.17 -12 | 1.17 -12 | 1.19 -12 | 1.17 -12 |
| 15 | 1.03 -12 | 1.08 -12 | 1.08 -12 | 1.07 -12 | 1.07 -12 | 1.07 -12 | 1.07 -12 | 1.07 -12 | 1.09 -12 | 1.07 -12 |
| 16 | 9.01 -13 | 9.33 -13 | 9.38 -13 | 9.27 -13 | 9.28 -13 | 9.26 -13 | 9.27 -13 | 9.26 -13 | 9.42 -13 | 9.29 -13 |
| 17 | 8.10 -13 | 8.32 -13 | 8.36 -13 | 8.27 -13 | 8.28 -13 | 8.27 -13 | 8.28 -13 | 8.27 -13 | 8.41 -13 | 8.29 -13 |
| 18 | 7.61 -13 | 7.77 -13 | 7.80 -13 | 7.72 -13 | 7.72 -13 | 7.71 -13 | 7.72 -13 | 7.71 -13 | 7.85 -13 | 7.73 -13 |
| 19 | 7.27 -13 | 7.38 -13 | 7.41 -13 | 7.33 -13 | 7.34 -13 | 7.33 -13 | 7.33 -13 | 7.33 -13 | 7.45 -13 | 7.35 -13 |
| 20 | 6.90 -13 | 6.97 -13 | 6.99 -13 | 6.92 -13 | 6.92 -13 | 6.92 -13 | 6.92 -13 | 6.92 -13 | 7.04 -13 | 6.94 -13 |
| 21 | 6.24 -13 | 6.27 -13 | 6.29 -13 | 6.23 -13 | 6.24 -13 | 6.23 -13 | 6.23 -13 | 6.23 -13 | 6.34 -13 | 6.25 -13 |
| 22 | 5.37 -13 | 5.37 -13 | 5.39 -13 | 5.34 -13 | 5.34 -13 | 5.33 -13 | 5.34 -13 | 5.34 -13 | 5.43 -13 | 5.35 -13 |
| 23 | 4.16 -13 | 4.15 -13 | 4.16 -13 | 4.13 -13 | 4.13 -13 | 4.12 -13 | 4.12 -13 | 4.12 -13 | 4.19 -13 | 4.13 -13 |
| 24 | 3.11 -13 | 3.09 -13 | 3.10 -13 | 3.07 -13 | 3.07 -13 | 3.07 -13 | 3.07 -13 | 3.07 -13 | 3.12 -13 | 3.08 -13 |
| 25 | 1.14 -13 | 1.13 -13 | 1.13 -13 | 1.12 -13 | 1.12 -13 | 1.12 -13 | 1.12 -13 | 1.12 -13 | 1.14 -13 | 1.13 -13 |

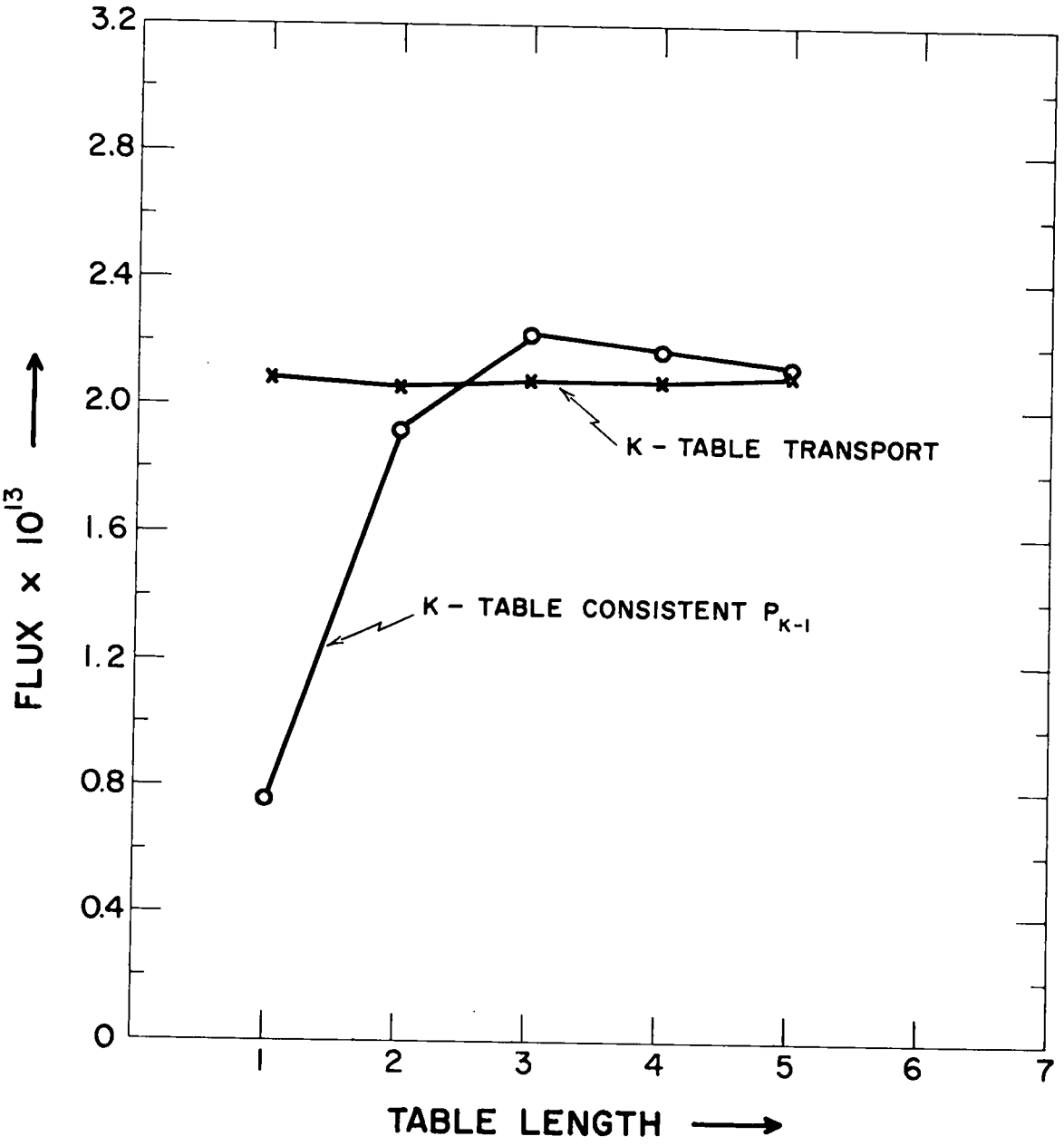


Fig. VI-1. Neutron flux gp 1 (12-14 MeV) in sea level air at R = 825 meters due to spherical volume source R = 10 meters, 1 neutron gp 1 (12-14 MeV). Comparison of different multitable approximations.

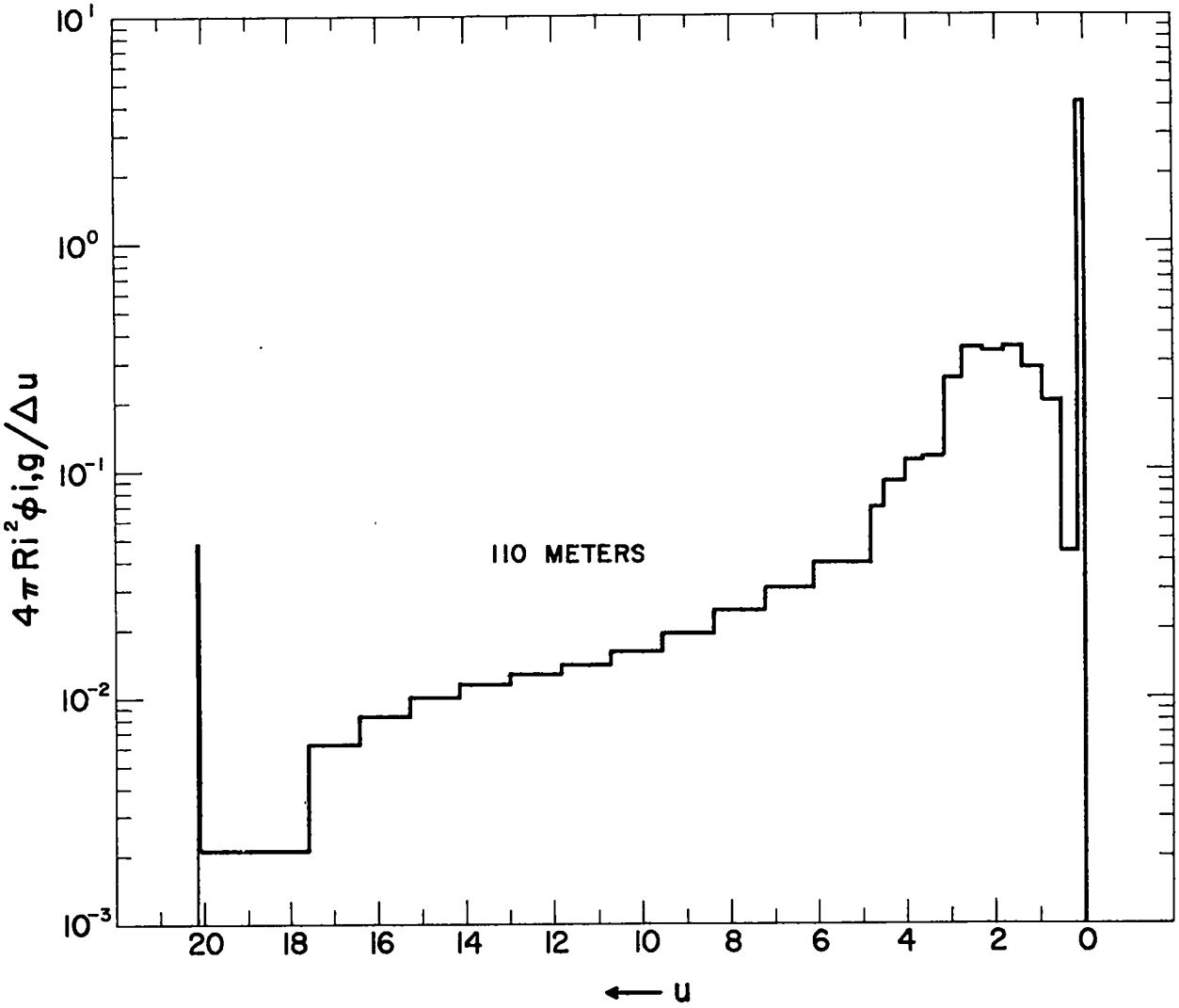


Fig. VI-2. Neutron spectrum from spherical volume source, R = 10 meters, 1 neutron of energy gp 1 (12-14 MeV) in sea level air at 110 meter distance.

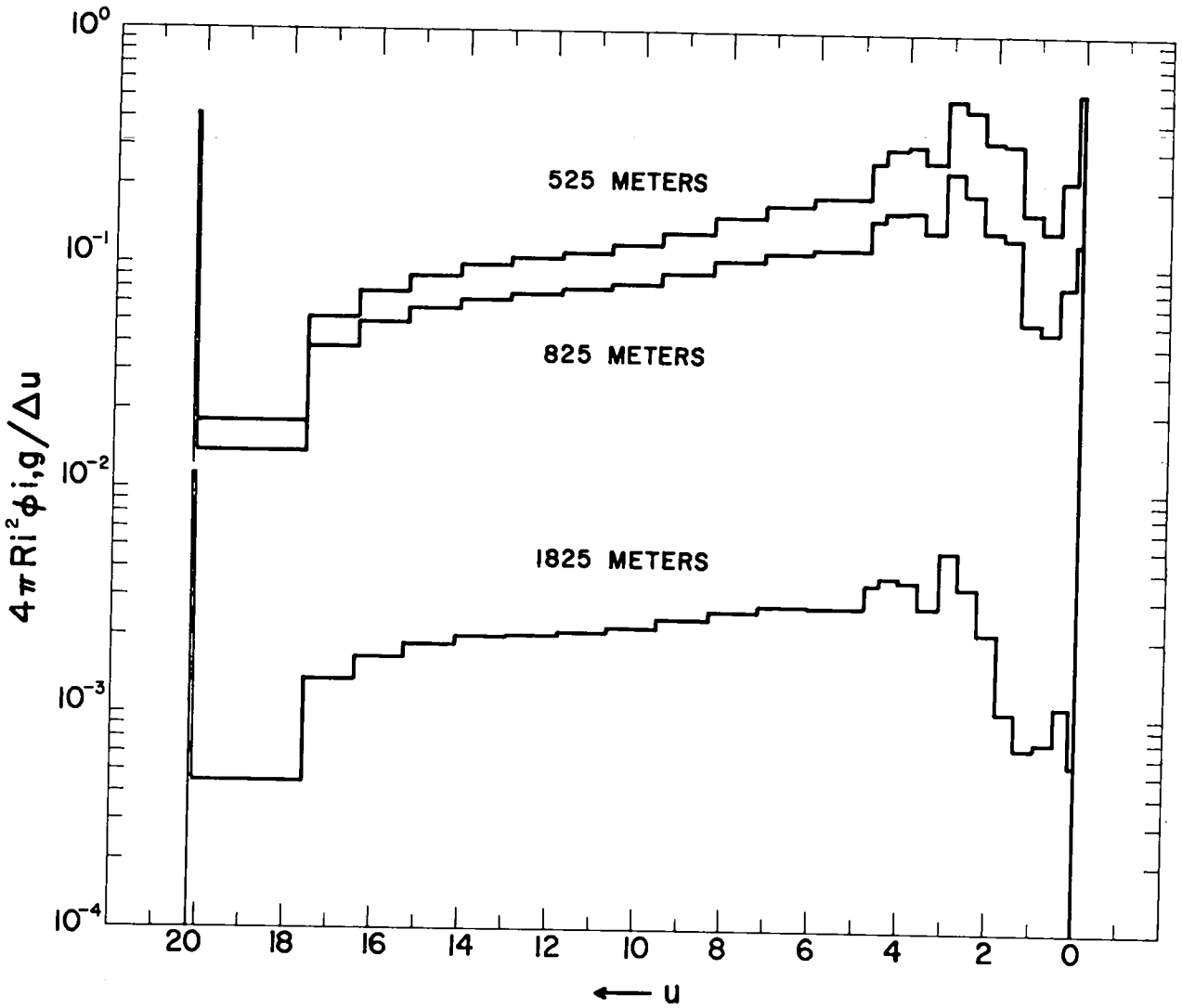


Fig. VI-3. Neutron spectrum from spherical volume source, R = 10 meters, 1 neutron of energy gp 1 (12-14 MeV) in sea level air at 525, 825 and 1825 meter distance.

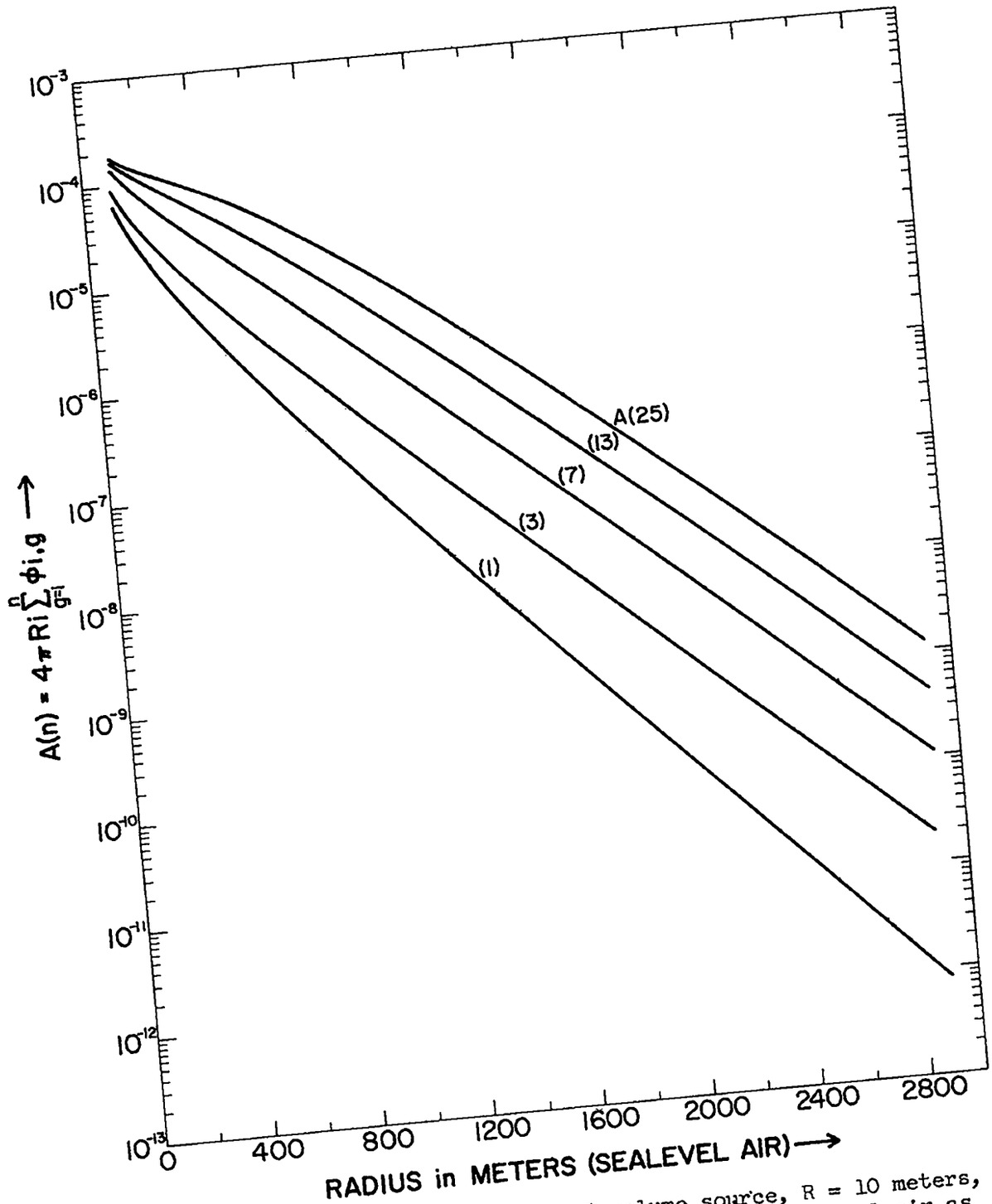


Figure VI-4. Neutron flux from spherical volume source, R = 10 meters, 1 neutron of energy gp 1 (12-14 MeV) in sea level air as a function of distance.

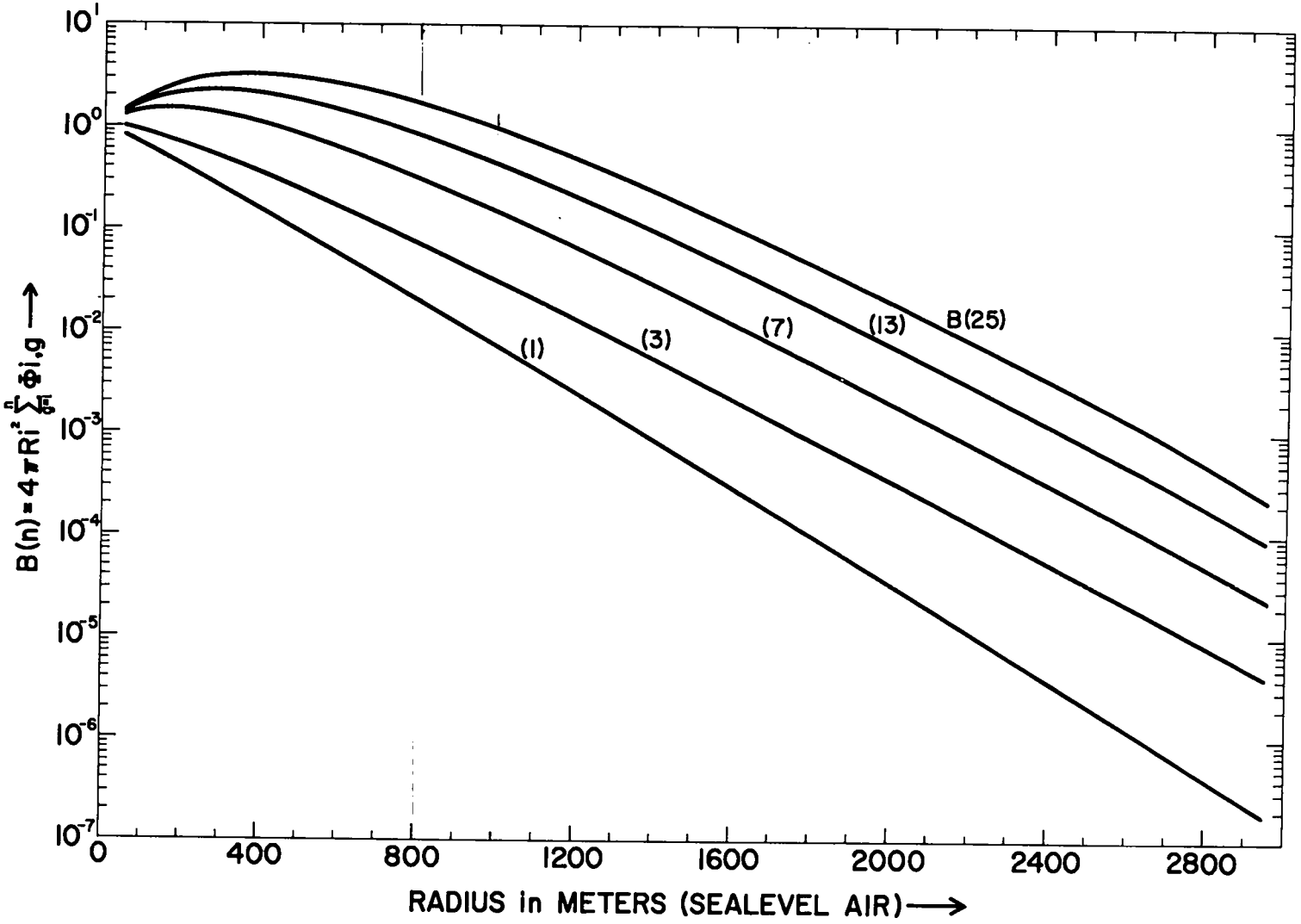


Fig. VI-5. Neutron flux from spherical volume source, R = 10 meters, 1 neutron of energy gp 1 (12-14 MeV) in sea level air as a function of distance.